Transport and precipitation of carbon and sulphur in the Reykjanes geothermal system, Iceland

E. Kevin Padilla Rivas

Faculty of Earth Sciences
University of Iceland
2011

Transport and precipitation of carbon and sulphur in the Reykjanes geothermal system, Iceland

E. Kevin Padilla Rivas

60 ECTS thesis submitted in partial fulfillment of a
Magister Scientiarum degree in Geology (Geochemistry)

Advisors
Andri Stefánsson, University of Iceland
Thráinn Fridriksson, Iceland Geosurvey

Faculty of Earth Sciences
School of Engineering and Natural Sciences
University of Iceland
Reykjavik, May 2011

Transport and precipitation of carbon and sulphur in the Reykjanes geothermal system, Iceland
Carbon and sulphur in the Reykjanes geothermal system
60 ECTS thesis submitted in partial fulfillment of a *Magister Scientiarum* degree in Geology (Geochemistry)

Faculty of Earth Sciences
School of Engineering and Natural Sciences
University of Iceland
Askja, Sturlugötu 7
101, Reykjavik
Iceland

Telephone: 525 4000

Bibliographic information:
E. Kevin Padilla, 2011, Transport and precipitation of carbon and sulphur in the Reykjanes geothermal system, Iceland, Master's thesis, Faculty of Earth Sciences, University of Iceland, pp. XX.

ISBN XX

Printing: XX
Reykjavik, Iceland, May 2011

Abstract

Sulphur and carbon analyses of drill cuttings, mineral saturation state calculations and reaction path modelling were used to assess the effects of boiling and phase separation, cooling, magmatic gas input and extent of fluid-rock reaction in order to get insight into the source, transport and precipitation of sulphur and carbon and associated metals in the Reykjanes geothermal system. Reservoir temperatures range from 275 to 310°C and the estimated pH from ~4.5 to ~5.0 with uncertainties up to 0.5 pH units. Geothermal reservoir waters seem to be the formed upon mixing of seawater with very small amount of magmatic gas followed by reaction with basalts. The reservoir water is relatively close to saturation with respect to most minerals observed in the system including quartz, albite, chlorite, epidote, prehnite and pyrite. Carbon dioxide concentrations in the reservoir water are close to an apparent equilibrium with the clinozoisite-calcite-quartz-prehnite mineral assemblage but CO_2 may also be source controlled by magmatic input corresponding to about 0.1 to 1 wt% magmatic gas to seawater ratio. The H_2 and H_2S concentrations are considered to be controlled by the buffer pyrite-prehnite-magnetite-quartz-clinozoisite-anhydrite or pyrite-wollastonite-magnetite-anhydrite-quartz. Carbon content in drill cuttings notably increases from ~0.01 to ~2.0 wt% as depth decreases in the uppermost 1100 m. Below that depth, concentrations range from <0.5 ppm to a maximum of ~0.03 wt%. At reservoir conditions, carbon precipitation may be precluded, due to the effects of temperature, pH and reduced availability of cations, and leaching from rocks seems to occur. Calcite precipitates and builds up in the altered rocks above background carbon at depths <1100 m, corresponding to depth of boiling. Sulphides concentrations range from <0.01 to ~1.2 wt% in altered rocks with no markable trend as a function of depth. Reservoir water with metal concentrations based on downhole samples was observed to be supersaturated with respect to most sulphide minerals and become increasingly more supersaturated upon boiling and cooling, in addition to sulphide being quantitatively removed from solution upon boiling mostly into pyrite but also sphalerite, galena and covellite. Under these conditions, sulphide minerals have the potential to form both in the reservoir and upon fluid ascent resulting in homogeneous sulphide precipitation as a function of depth. Sulphates in rocks range from ~0.02 to 1.8 wt%, with the highest values observed in the uppermost 400 m. Anhydrite precipitation occurs preferentially in the shallowest part of the system mainly due to heated seawater-rock interaction. Total sulphur vertical distribution pattern at Reykjanes may reflect either significant sulphides precipitation at all depths due to high metal concentrations in the reservoir water or enhanced sulphur precipitation due to additional sulphur supply from seawater intruding at all depths, or both. Finally, based on age and extension constrains for the geothermal system, average mass of mineralization of 700, 315 and 1054 tonne/yr were obtained for sulphide, sulphate and carbon, respectively, over the life time of the system taken to be 20000 years.

Útdráttur

Í þessari rannsókn voru efnagreiningar á brennisteini og kolefni í borholusvarfi, útreikningar á mettunarástandi jarðhitasteinda í djúpvöka og líkanreikningar sem herma efnahvörf milli vatns og bergs notuð til að leggja mat á hvernig áhrif suðu, aðskilnaður gufu frá vatni og kæling, efnahvörf milli vatns og bergs og gasflæði frá kviku hafa áhrif á flutning brennisteins og kolefnis í jarðhitakerfinu á Reykjanesi og útfellingu málmsteinda. Djúphiti á Reykjanesi er á bilinu 275-310°C og pH á vatni í æðum er ~4,5 til ~5,0 með óvissu sem nemur allt að 0,5 pH einingum. Djúpvatnið er sjór með örlítilli blöndun við kvikugös sem hefur hvarfast við basalt. Djúpvatnið reiknast fremur nálægt efnajafnvægi við allar greindar ummyndunarsteindir, þ.á.m. kvars, albít, klórít, epídót, prenít og pýrít. Styrkur koltvíoxíðs í djúpvökva er nálægt jafnvægi við steindafylkið klínósóisít-kalsít-kvars-prenít en styrkur koltvíoxíðs gæti einnig stjórnast af ístreymi frá kviku sem svarar til 0,1-1% af kvikugasi í jarðsjónum. Styrkur vetnis og brennisteinsvetnis í djúpvatni er talinn ráðast af efnajafnvægi við steindafylkið pýrít-prenít-magnetít-kvars-klínósóisít-anhýdrít eða fylkið af pýrít-vollastónít-magnetít-anhýdrít-kvars. Kolefnisinnihald í borholusvarfi eykst greinilega frá ~0,01 til 2,0 % miðað við þunga með minnkandi dýpi ofan 1100 m. Neðan þessa dýpis er styrkurinn frá <0,5 ppm upp í 0,03%. Í djúpæðum er mögulegt að útfelling kolefnissteinda eigi sér ekki stað vegna ríkjandi hita, pH-gildis og takmörkuðu framboði katjóna sem bindast kolefninu. Útfellingar kalsíts verða í ummynduðu bergi ofan 1100 m eða dýpis sem samsvarar því dýpi þar sem áköf suða hefst. Styrkur súlfíðsteinda liggur á bilinu <0,01% til ~1,2% miðað við þunga. Engin regluleg breyting með dýpi er sjáanleg. Styrkur málma í djúpvatni samkvæmt efnagreiningu á djúpsýnum svaraði til yfirmettunar m.t.t. flestra súlfíðsteinda og yfirmettunin vex við suðu og samsvarandi kælingu vatnsins umfram upphaflega yfirmettun. Mestur hluti súlfíðs sem tapast úr vatninu fer í það að mynda steindina pýrít en einnig svalerít, galena og kóvellít. Við ofangrein skilyrði geta súlfíðsteindir myndast bæði í djúpvökva og í uppstreymisrásum þar sem suða á sér stað. Þetta leiðir til þess að magn súlfíðsteinda í berginu er ekki háð dýpi. Styrkur súlfats í ummyndaða berginu er á bilinu 0,02-1,8% miðað við þunga. Hæstu gildin eru í efstu 400 m jarðhitakerfisins. Útfelling anhýdríts verður einkum efst í jarðhitakerfinu vegna þess að ekki þarf að hita sjó mikið áður en anhýdrít-mettun næst. Dreifing á styrk heildarbrennisteins með dýpi í Reykjaneskerfinu gæti orsakast af útfellingu súlfíðsteinda á öllum dýptarbilum vegna hás styrks málmsteinda í jarðhitavatninu eða aukinni útfellingu brennisteins úr vatninu vegna aukins framboðs af brennisteini sem verður við írennsli sjávar í kerfið á hvaða dýpi sem er eða hvorutveggja. Á grundvelli aldurs jarðhitakerfisins og stærðar þess nemur árleg útfelling sulfíð-, súlfat- og karbónatsteinda 700, 315 og 1054 tonnum yfir líftíma kerfisins sem metinn var 20.000 ár.

For Olga and Evelin

Table of Contents

List of Figures

List of Tables

Acknowledgements

My sincere gratitude to the United Nations University Geothermal Training Program for awarding the scholarship and to its staff Dr. Ingvar Fridleifsson, Mr. Ludvík Georgsson, Ms. Thorhildur Isberg, Ms. Dorthe Holm, Mr. Ingimar Haraldsson and Mr. Markus Wilde for providing enormous help that made possible for me to complete my studies. To my advisors Andri Stefánsson and Thráinn Fridriksson for letting me work in this project, for their great support and guidance and for teaching me many things both on science and life. To my collegues, Alejandro Rodríguez, Hanna Kaasalainen, Nicole Keller, Ása Sigurdardóttir, Sam Scott, Júlia Börke, Eygló Ólafsdóttir, Gro Birkefeldt, Iwona Galeczka, Jonas Olsson, Helga Hilmarsdóttir, Helgi Alfredsson and Sigurdur Markusson for fruitful discussions and support in many aspects. To Saedís Ólafsdóttir, Signý Gunnarsdóttir and Rósa Jónsdóttir for helping me with the laboratory work and to find scientific articles. To Prof. Stefán Arnórsson and Dr. Jón Örn Bjarnasson for helpful discussions. Finally, to my family for their infinite patience and support during my staying abroad.

1 Introduction

Natural geothermal systems are found where a body of hot rock and/or magma, fluid and permeability coexist. Geothermal systems have been classified into volcanic or high-temperature and non-volcanic or low-temperature geothermal systems (Bödvarsson, 1961; Nicholson, 1993; Goff and Janik, 2000; Arnórsson et al., 2007). Non-volcanic systems are associated with a body of hot rock and occurring in various geological settings like areas that are tectonically active. Volcanic geothermal systems are, on the other hand, associated with active volcanism and magmatic heat. Reported measured aquifer temperatures range from ambient to over 400°C and depending on the temperature and pressure conditions, they may be either single phase or two phases (Arnórsson et al., 2007). Sub-boiling systems are single liquid phase whereas volcanic geothermal systems are either liquid dominated (liquid and vapour) or vapour dominated (almost pure vapour) (White et al., 1971; Nicholson, 1993).

Geothermal fluids have been divided according to their origin into primary and secondary fluids. Primary geothermal fluids are those found at the bottom of the convection cell (reservoir) whereas secondary fluids are produced from primary fluids upon processes occurring on their ascent to the surface, including fluid mixing and phase separation. Examples of primary fluids are sodium-chloride waters, acid sulphate-chloride waters and brines whereas secondary geothermal fluids include steam-heated acid sulphate waters, carbon dioxide waters and mixed waters (Ellis and Mahon, 1977; Arnórsson et al., 2007). Examples of the chemical composition of various types of primary and secondary geothermal fluids are shown in Table 1. Discussion on the origin of the chemicals in geothermal systems is still open, fluid-rock interaction and magma degassing probably being the main sources (e.g. Ellis and Mahon, 1964, 1967; Hedenquist and Lowestern, 1994; Giggenbach, 1992). Carbon and sulphur are among the major components in geothermal fluids and CO_2 and H_2S the most important gases.

Based on natural geothermal fluid composition it has been concluded that local equilibria between the geothermal minerals and fluids controls the concentration of major components, except mobile elements like chloride, at temperatures as low as 50°C (e.g. Ellis, 1970; Giggenbach, 1980, 1981; Arnórsson et al., 1983; Stefánsson and Arnórsson, 2000, 2002). The reason for this is twofold. Firstly, as demonstrated for Icelandic geothermal systems two types of fluids recharge the systems, saline and meteoric, yet despite the variable elemental concentrations, at a particular temperature the relative concentrations are the same with respect to major elements. Secondly, based on the Phase Rule and assuming pressure effects on the reactions to be insignificant, only two parameters are needed to describe a system, temperature and one component, notably Cl, concentration. The geothermal minerals commonly observed are generally also calculated to be saturated with respect to the fluids. They typically show strong temperature dependence but primary rock composition also plays a role.

Studies of Icelandic high temperature systems show a close relationship between the geothermal mineral assemblages with depth (Björnsson et al., 1972; Tómasson and Kristmannsdóttir, 1972; Kristmannsdóttir, 1975, 1976, 1979; Fridleifsson, 1991; Schiffman and Fridleifsson, 1991). Four distinct alteration zones have been suggested. At temperatures below 200°C zeolite and smectite predominates, replaced by mixed layer clay minerals and prehnite with increasing temperature. Epidote and chlorite become the

dominant sheet silicate at temperatures above 230°C characterizing the third alteration zone, whereas the appearance of amphibole marks the fourth one. Fluid salinity has minor effects on the geothermal zonation, yet, the fluid composition appears to affect how the minerals respond to differences in original rock composition. At Reykjanes, seawater appears to control the composition of the secondary minerals. On the other hand, at Krafla, the fluids are dilute and the composition of the alteration minerals appears to reflect more closely the parental rock composition (Sveinbjörnsdóttir et al 1986). In addition, Lonker et al. (1993) showed that the alteration minerals, mineral compositions and textures in two of the Icelandic geothermal systems (Reykjanes and Svartsengi) do not record a simple increase of temperature with depth. The study suggested that mineral and textural features can be correlated with fluid compositions, processes of fluid flow and mixing and formation permeability.

Geothermal altered rocks in upflow-boiling zones of high-temperature systems in Iceland are often enriched in sulphur and carbon (Björnsson et al., 1972; Gunnlaugsson, 1977). Sulphur concentration may be as high as 2-5 wt%, whereas in basaltic glass it is only 0.08 wt% and in holocrystalline basalt as low as 0.01-0.02 wt% (Gunnlaugsson, 1977). Carbon concentration in upflow zones may be as high as 1 wt% but in basalt it is about 0.012 wt% on average (Björnsson et al., 1972; Flower et al., 1982). The source of supply of the elevated sulphur and carbon concentrations in the boiling zones of high-temperature geothermal systems is considered to be the magmatic (e.g. Giggenbach, 1992). The enrichments, on the other hand, may be caused by the processes of gas-water-rock interaction including boiling, conductive cooling and/or mixing (Holland and Malinin, 1979; Fournier, 1985; Simmons and Christenson, 1994).

The most common sulphur containing minerals in geothermal systems are pyrite and pyrrhotite whereas carbon predominantly forms calcite (e.g. Browne, 1978). Calcite is observed at all depths to about 270-300°C in high temperature geothermal systems in Iceland. Its occurrence is variable, being more abundant in tuff and uppermost parts of the system (Tómasson and Kristmannsdóttir, 1972; Franzson et al., 2002). Pyrite has been observed associated with geothermal altered rocks in Iceland at temperatures between 100 and over 300°C and is found in veins with other precipitates and also dispersed in the groundmass of the rocks (Kristmannsdóttir, 1979). Pyrrhotite has been observed together with pyrite as a secondary mineral associated with dilute geothermal fluids, however, in the geothermal seawater systems at Reykjanes and Svartsengi, pyrrhotite is absent whereas anhydrite and magnetite are observed (Ragnarsdóttir et al., 1984; Lonker et al., 1993). Sphalerite, chalcopyrite and galena have also been observed but are less abundant than pyrite (Marks et al., 2010).

Geothermal fluids transporting metals are responsible for the formation of important ore deposits (e.g. Helgeson, 1970; Weissberg et al., 1979; Hedenquist and Lowenstern, 1994) particularly by formation of metal rich sulphides. The metals may be transported as free ions or hydroxyl complexes or complexed to sulphide and chloride ligands and upon cooling, boiling and mixing, the sulphides may precipitate (e.g. Barnes, 1979).

The aim of the present study is to get insight into the source, transport and precipitation of sulphur and carbon in the Reykjanes geothermal system and the associated metal transport and precipitation. Data on fluid discharge and deep liquid composition as well as sulphur and carbon concentrations in altered rocks were used together with various types of geochemical modelling to assess the possible magmatic input into the geothermal system, mass and composition of carbon and sulphur precipitated and the effects of various processes including boiling and cooling.

Table 1. Chemistry of the major types of primary (samples 1-10) and secondary (samples 11-13) geothermal waters. The concentrations of the major components are in mg/L and mg/kg.

Sample	1[a]	2[a]	3[b]	4[a]	5[b]	6[a]	7[a]	8[b]	9[a]	10[a]	11[a]	12[a]	13[a]
t_f (°C)	241	276	253	248		237	278		280	238	94	60	65
P_S	35.6	42	8.6	0		0	0		9.8	18.5			
pH/t (°C)	5.2/	5.16/	6.2/	8.1/	7.8	4.8/	3.1/	2.4	7.46/	8.8/	1.2	6.2/	8/
	20.9	22	20	25		25	25		20	18		25	26
Cl	23430	19251	8430	3026	3021	103000	6175	13400	113.1	73.5	1.2	85.8	20.7
SO_4	13.2	24.3	11.5	137.6	63	12	508	350	8.6	290.8	1598	41.3	19.9
Na	11912	10089	4831	1764	1710	38839	3117	5490	214.4	147	535	417.7	209.7
K	1833	1447	827	277	168	6250	950	900	43.8	18	78.3	30.6	35.9
Ca	1868	1637	194.2	68.4	32	20630	82	1470	0.8	2.4	56.1	99.7	10
Mg	1.5	1.075	0.2	0.2	0.2	34	25	131	0.049	0.0016	15.6	27.2	1
Fe	4.1	0.293			0	4.4	282	220	0.027	0.0026	37.6	1.5	0.017
Al	0.1	0.045							1.08	0.969	27.5	0.04	0.0094
SiO_2	816	672	799.8	361	270	550	910	639	815	500	182	212	176.2
B	10.1	6.718	160.1	30	90		21	106	1.73	0.105		0.5	0.4
F	0.3	0.138			1.7	4		7	1.36	1			4.6
CO_2	60.3	47.4	2.3	27.7	2[c]	54.8	0	0	200.6		0	1145	300.6
H_2S	4	3.4		0			0		53.5			<0.01	0
Trace components													
Cu		1.74								0.18	4	<1.0	0.09
Zn		50.9								0.51	134.5	0.5	3.2
Pb		<0.1								<0.01	8.1	<0.1	0.173
As		156											

[a] in mg/L; [b] in mg/kg; [c] as HCO_3; t_f: aquifer temperature; P_S: sampling pressure in bar-g

1: Volcanic, seawater geothermal system in basalt, Reykjanes, well 10, Iceland (ISOR , 2006, unpublished data)

2: Volcanic, seawater geothermal system in basalt, Reykjanes, well 15, Iceland (Arnórsson et al., 2007)

3: Andesitic-basaltic volcanic geothermal system, Berlín, wet-steam well 17, El Salvador (Renderos, 2002)

4: Andesitic volcanic geothermal system, Momotombo, well 2, Nicaragua (Arnórsson, 1997)

5: Taumatapuhi Geyser, Tokaanu, New Zealand (Ellis and Mahon, 1977)

6: Na-Ca-Cl brine, Assal, Djibouti, (D´Amore et al., 1998)

7: Acidic sulfate-chloride water, Mahanagdong, well 9, Leyte, Philippines (Arnórsson et al., 2007)

8: Well 205, 1500 m deed, Matsao, Taiwan (Ellis and Mahon, 1977)

9: Volcanic geothermal system in basalt, Krafla, well 20, Iceland (Gudmundsson and Arnórsson, 2002)

10: Volcanic geothermal system in basalt, Krafla, well 21, Iceland (Arnórsson et al., 2007)

11: Steam-heated surficial acid sulfate water, Mendeleev, Kunashir, Russia (Chelnokov, 2004)

12: Carbon dioxide water, Lýsuhóll well 6, Iceland (Arnórsson et al., 2007)

13: Mixed high temperature and cool ground water, Nedridalur, Geysir field, Iceland (Arnórsson et al., 2007)

2 The Reykjanes geothermal system

2.1 Geological settings

The Reykjanes geothermal system is located on the Reykjanes Peninsula, SW Iceland (Figure 1). It is constructed of young, highly permeable basaltic formations, transacted by an intense NE-SW trending fault zone, and is tectonically active (Björnsson et al., 1970). The volcanic activity on the peninsula is concentrated along five distinct fissure swarms, but central volcanic complexes are notably absent from the four westernmost ones (Jakobsson et al., 1978). High temperature geothermal systems occur in all of the Reykjanes Peninsula fissure swarms.

The Reykjanes geothermal area seats at the centre of swarms of active faults that facilitate hydrologic convection. High-level magma chambers have apparently not formed in the Reykjanes volcanic systems (Gudmundsson and Thórhallsson, 1986), and sheeted dike complexes are likely to serve as the magmatic heat source for the geothermal activity. Surface geothermal manifestations occurs over an area of ~1 km^2, but observations from more than 30 drill holes and several resistivity surveys indicate that the subsurface area of the active system is at least 2 km^2 consistent with the findings of Björnsson et al. (1972) and Pálmason et al. (1985).

2.2 Stratigraphy, alteration mineralogy and temperature

The stratigraphy of the Reykjanes geothermal system is divided into two informal formations. The uppermost 1000 m of the geothermal system are characterized by hyaloclastite tuffs, breccias, tuffaceous and marine sediments whereas the deeper part is dominated by subaerial basaltic lavas (Björnsson et al., 1972; Tómasson and Kristmannsdóttir, 1972; Lonker et al., 1993; Franzson et al., 2002; Marks et al., 2010).

Reaction of geothermal fluids with the basaltic host rock has formed a series of progressively higher alteration zones with depth observed in the geothermal system, each zone characterized by distinct mineral assemblages and categorized based on key index minerals (Figure 2). In order of increasing alteration grade the zones are as follows: mixed-layer smectite–zeolite, epidote-mixed-layer clay, chlorite-epidote and epidote-actinolite (Tómasson and Kristmannsdóttir, 1972; Lonker et al., 1993; Franzson et al., 2002; Fridleifsson and Elders, 2005; Marks et al., 2010).

Calcite is most abundant in the smectite-zeolite and the chlorite zones, and observed sporadically throughout the chlorite-epidote zone. It is typically absent, or occurs in trace quantities in the deeper portions of the epidote-actinolite zone, where temperature exceed 300°C (Freedman et al., 2009). Of the sulphide minerals found at Reykjanes, pyrite is the most abundant and it is present at all depths in small amounts (Tómasson and Kristmannsdóttir, 1972). Anhydrite is observed sporadically (Lonker et al., 1993; Franzson et al., 2002; Marks et al., 2010).

Franzson et al. (2002) studied the mineral deposition sequence in samples from the well RN-10. The results are summarized in Figure 3. At depths <600 m, smectite linings fall nearest to the wall of the voids, and then succeeded by aragonite, chalcedony (possibly

initially deposited as opal) and zeolites. The youngest depositions are calcite and anhydrite. Below 600 m, possible anhydrite is succeeded by chlorite, prehnite, quartz and minor calcite. Pyrite, epidote and wollastonite are found at similar episodes of precipitation and amphibole and quartz are the youngest depositions. According to these observations, the geothermal system is moving toward higher temperatures.

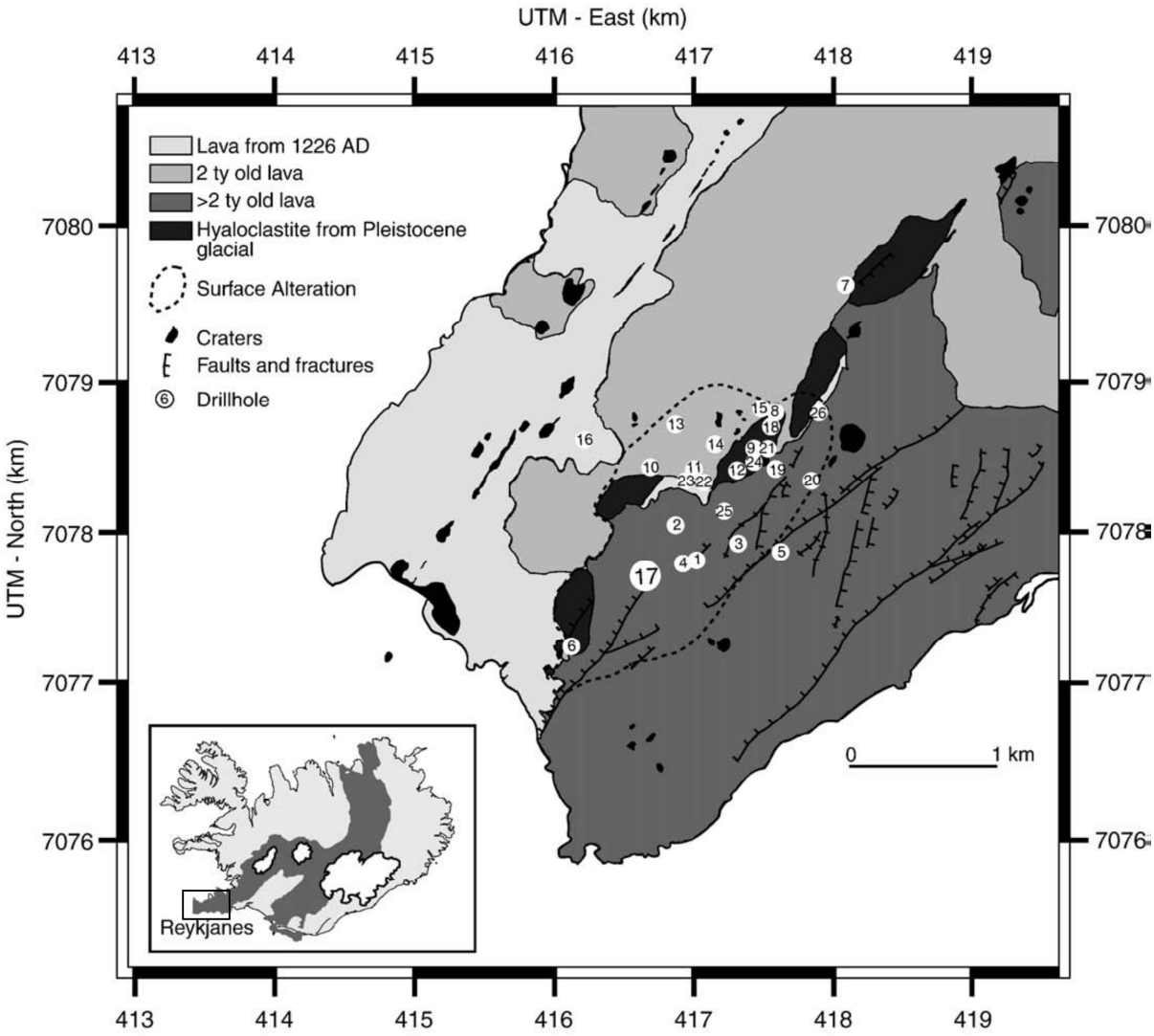

Figure 1. The Reykjanes geothermal area, Reykjanes Peninsula, Iceland (after Freedman et al., 2009).

2.3 Fluid chemistry

At present, the Reykjanes geothermal water represents heated seawater without any freshwater mixing (Arnórsson, 1978), however, fluid inclusion studies on borehole cuttings and stable isotope ratios of geothermal fluids and secondary minerals indicate that dilute fluids dominated the system at earlier times (Sveinbjörnsdóttir et al., 1986; Franzson et al., 2002; Pope et al., 2009). The difference in the composition of seawater and the geothermal water is due to interaction with the basaltic host rocks at elevated temperatures, with the geothermal water enriched in SiO_2, K, Ca and depleted in SO_4 and Mg but with same Cl concentration as seawater (Björnsson et al., 1970, 1972; Arnórsson, 1978, 1983). Depth versus pressure and temperature profiles indicates that geothermal fluids in the Reykjanes

system are boiling in the uppermost 1000 to 1300 m of the system (Franzson et al., 2002; Hardardóttir et al., 2009).

The Reykjanes geothermal system has been identified an as active ore-forming system (Hardardóttir et al., 2001). Scales enriched in metals are common in pipelines at Reykjanes and they include the minerals sphalerite, bornite, digenite, galena, chalcopyrite, native silver, silver sulphides, gold (probably occurring in solid solutions or as submicroscopic inclusions) and pyrite among others, with abundances varying from well to well due to differences in physical parameters of the wells (Hardardóttir et al., 2010). Copper, Zn, Pb, Fe, Ag, Au, As and S concentrations in scales are as high as 26.3 wt%, 26.7 wt%, 16.7 wt%, 20 wt%, 2.3 wt%, 589 ppm, 175 ppm and 28 wt% respectively and the highest metals concentrations (except for Fe) are found in the wells RN-12, RN-21 and RN-24 where extensive boiling occurs due to a sharp pressure decrease over a distance of few centimetres in surface pipes at an throttle point (Hardardóttir et al., 2010).

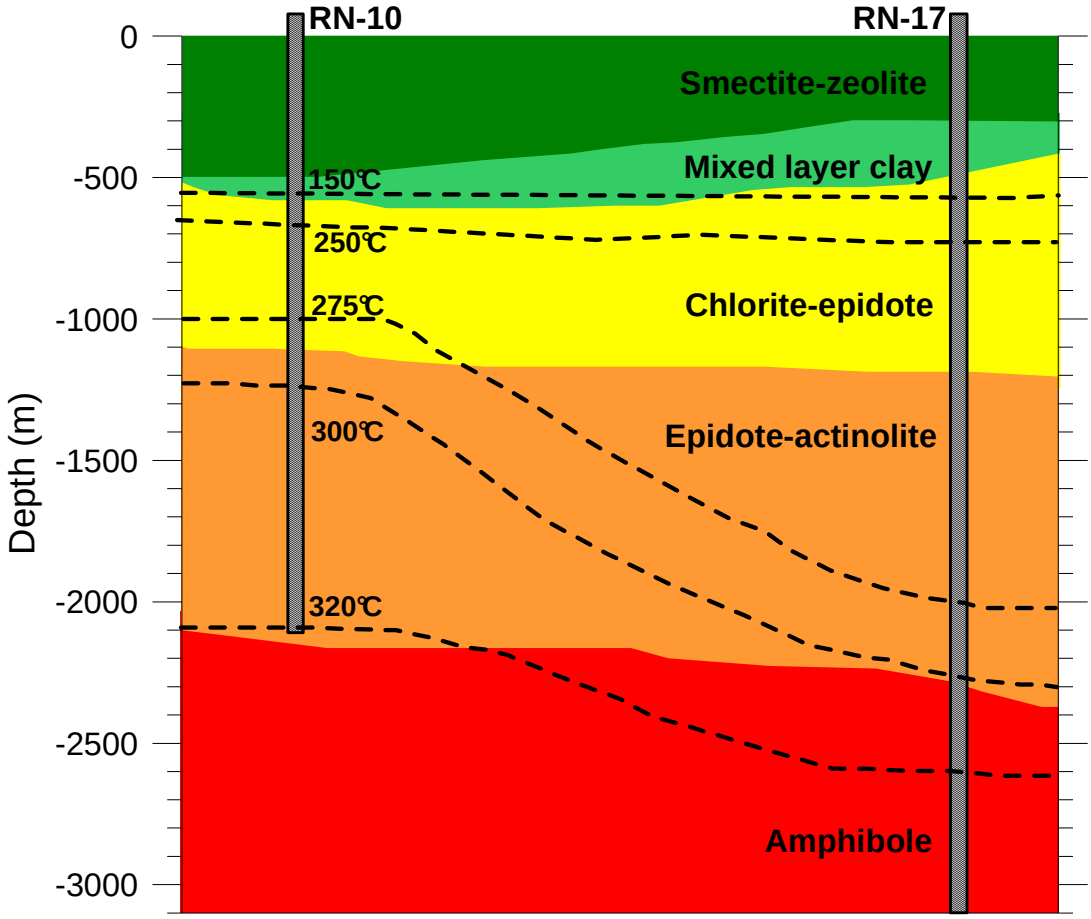

Figure 2. Hydrothermal alteration zones and temperatures identified in the Reykjanes geothermal system (Modified from Franzson et al., 2002 and Marks et al., 2010). Isotherms shown are based on measured temperatures in wells number RN-10 and RN-17. Alteration zones are consistently observed in the geothermal system.

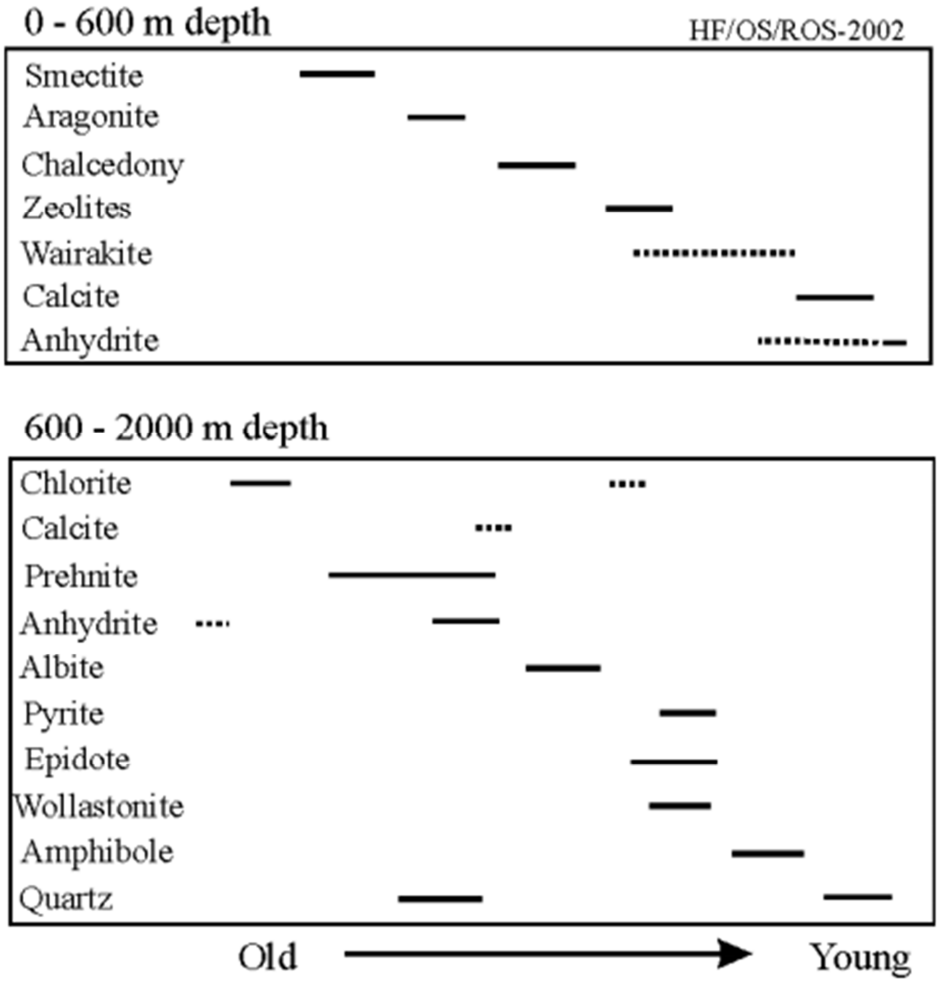

Figure 3. Probable time sequence of mineral deposition in well RN-10 (after Franzson et al., 2002).

3 Methods

3.1 Total carbon, total sulphur, sulphides and sulphates analysis in drill cuttings

Total carbon, sulphide sulphur, sulphate sulphur and total sulphur concentrations were analysed in 80 samples of drill cuttings from two geothermal wells at Reykjanes, number RN-10 and RN-17. The samples analysed were collected at ca. 50 m depth intervals, from 100 m to 2051 m for well RN-10 and from 100 m to 3050 m for well RN-17. The wells RN-10 and RN-17 were selected as the former is the one with the highest downhole measured temperature and the latter is the deepest well that has been drilled in the area, in addition these wells have been extensively studied for alteration mineralogy and composition (e.g. Franzson et al., 2002; Freedman et al., 2009; Pope et al., 2009; Marks et al., 2010).

The fresh drill cuttings samples were washed with deionised water to clean out fine material from the drilling mud. In some cases, visible flakes, assumed to be iron oxides coming from the drill bit, were manually removed. Around 20 g of the drill cuttings samples were ground to fine powder using a carbide ball mill. The fine powder was used both for the carbon and sulphur analysis.

Total carbon was measured using a carbon analyser from UIC Inc. Coulometrics. A known mass (20±3 mg) was weighed into a tin boat and combusted in oxygen at 950-1000°C to convert all carbon in the sample to CO_2(g). The sample combustion gases were swept through a barium chromate scrubber to ensure complete oxidation of carbon to CO_2. Moreover, a series of chemical scrubbers were used to remove all non-carbon combustion products from the gas stream. The CO_2-containing gas stream was passed into a cell filled with a solution containing monoethanolamine and a colorimetric pH indicator. This acid causes the colour indicator to fade. A photodetector monitors the change in the colour of the solution as percent transmittance (%T). As the %T increases the titration current is automatically activated to an electrochemically generated base at a rate proportional to the %T. When the solution returns to its original colour (original %T), the current is terminated. The Coloumeter is based on the principles of Faraday´s Law. Each faraday of electricity expended is equivalent to 1 gram equivalent weight of CO_2 titrated. The CO_2 content is expressed as mass of total carbon and by knowing the total mass of the sample, the weight percentage of carbon can be calculated. Measurements in calcite standards (reagent purity) containing 100% (10 standards) and 50% calcite (4 standards) equivalent theoretically to 12 wt% and 6 wt% carbon, respectively, were carried out to verify the accuracy and precision of the instrument. The arithmetic mean obtained for the 12 wt% C standards was 11.83 wt% C and 5.89 wt% C for the 6 wt% C standard, indicating an acceptable accuracy and precision of the analysis.

Total sulphur, sulphide and sulphate were determined using a LECO® CS-400 Carbon/Sulphur analyser. The equipment utilizes a 2.2kW induction furnace coupled with an infrared absorption cell. The sample is combusted with oxygen in the induction furnace adding 2 g of tungsten trioxide as a combustion accelerator. As a result, the sulphur in the sample is oxidized to SO_2. The combustion gases are carried by oxygen into the infrared (IR) cell where sulphur is detected as SO_2. The determination of sulphur is done by non-

dispersive (fixed) infrared energy at precise wavelengths as the gases pass through their respective IR absorption cells. The changes in energy are then observed at the detectors and the concentration is determined. The process described above for sulphur measurement is known as the LECO method and its detection limit is 0.01 wt%.

The determination of total sulphur (TS), sulphide + sulphate (SS), and sulphate only (S^{6+}) is done in 3 different steps (Table 2). For each sample of pulverized drill cuttings, a mass of about 0.1 g was precisely weighed in triplicate into preheated crucibles. Firstly, total sulphur is measured in the sample following the procedure described above (the LECO method) without any previous treatment of the sample. Secondly, in order to measure sulphide + sulphate (SS) a previous step is needed to remove elemental sulphur from the sample. For this purpose, the second weighed sample is pre-treated by placing it into an electric kiln preheated to 288°C for one hour. The remaining sulphur is then measured by the LECO method (as total sulphur) and the result obtained in this way accounts for sulphate + sulphide sulphur in the sample. As a third step, sulphate sulphur (S^{6+}) is measured. The third weighed sample is placed into an electric kiln and preheated to 649°C for one hour. This is done in order to remove sulphide sulphur in addition to elemental sulphur from the sample. Sulphur is then measured by the LECO method and the result accounts only for sulphate sulphur. To determine sulphide sulphur (S^{2-}), measured sulphate sulphur was subtracted from sulphide + sulphate (SS) to give total sulphide, i.e. $S^{2-} = SS\text{-}S^{6+}$.

In order to verify the linearity of the instrument, a set of standards with different known concentrations were prepared from natural mineral samples and analysed for sulphide and sulphate. The results are shown in Figure 4. The comparison of measured versus expected concentrations of sulphide and sulphate in standard samples. demonstrate a satisfactory linearity. The most significant source of error may be attributed to the process of weighing relatively small amounts of the components during the preparation of the standards.

Table 2. Sample pre-treatment for sulphur analysis and speciation in rock samples.

Pre-treatment	Species removed	Species measured
None	None	Total sulphur (TS)
288°C, 1 hour	Elemental sulphur (ES)	Sulphide and sulphate (SS)
649°C, 1 hour	Elemental sulphur (ES) + sulphide (S^{2-})	Sulphate (S^{6+})

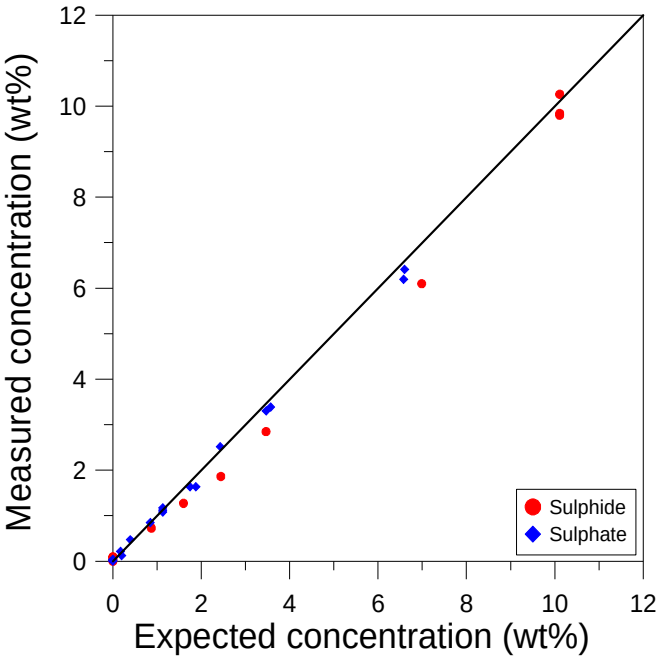

Figure 4. The comparison of measured versus expected concentrations of sulphide and sulphate in standard samples.

3.2 Calculation of geothermal reservoir water composition, aqueous speciation, mineral saturation state, boiling, cooling and reaction path modelling

The WATCH speciation program version 2.4 (Bjarnason, 1994), was used to estimate the component concentrations in the geothermal reservoir water, sometimes referred as "aquifer" or "deep liquid", based on chemical analyses of water and steam samples collected from discharging wells. In the calculation of aquifer water composition it is assumed that no transfer of heat or mass occur on the way from the reservoir to the surface, i.e. the system was assumed to be isolated (Arnórsson et al., 2007). It follows that,

$$H^{d,t} = H^{f,t}$$

$$m_i^{f,t} = m_i^{d,t} = m_i^{d,l}\left(1 - x^{d,v}\right) + m_i^{d,v}\, x^{d,v}$$

where H, m_i and x designate enthalpy, concentration of the *i-th* component and vapour fraction, respectively, *d* and *f* are the discharge and feeding aquifer, respectively and *l, v and t* denotes liquid, vapour and total, respectively. Further, it is assumed that the total discharge enthalpy is the same as that of steam saturated water at the aquifer temperature. The selected reference temperatures used for the calculations are based on downhole measurements and quartz geothermometry and they range from 275 to 310°C. In addition, closed system boiling and conductive cooling calculations were performed using the WATCH program in order to evaluate the effects of boiling and phase separation and cooling on the potential precipitation of carbon and sulphur minerals.

Aqueous speciation and mineral saturation states were calculated, both for aquifer fluids and in boiling and cooling modelling, based on the component concentration obtained from WATCH program and using the Lawrence Livermore National Laboratory database (llnl.dat) and the USGS WATEQ database (wateq4f.dat). Both these databases are applicable to ~300°C at water vapour saturation pressure and include major and trace dissolved species and minerals found in the Reykjanes system. The purpose of using the two databases was to compare the results and study the effects and possible errors using various sources of thermodynamic data. The databases were updated in the present study to include data on Au-OH, Au-Cl and Au-HS complexes as well as Cu-HS and Zn-HS complexes (Mountain and Seward, 2003; Stefánsson and Seward, 2003a,b,c, 2004; Tagirov and Seward, 2010). A summary of the types of complexes included in the calculations are given in Table 3.

In addition, the equilibrium mineral solubilities were updated, as far as possible, in the present study (Table 4) and they are based on values reported by Arnórsson and Stefánsson, (1999) Gunnarsson and Arnórsson (2000) and Stefánsson et al. (2009, 2011) and calculated using the Supcrt92 program (Johnson et al., 1992) and include secondary minerals observed in the Reykjanes geothermal system (Kristmannsdóttir, 1979; Lonker et al., 1993; Franzson et al., 2002; Freedman et al., 2009; Marks et al., 2010).To gain further insight into gas-water-rock interaction and the effects of gas (acid) supply and source of carbon and sulphur to the system, additional reaction path simulations were conducted using the and PHREEQC program (Parkhurst and Appelo, 1999) and the llnl.data database. The calculations involved reaction path modelling of seawater with basalts at 300°C and water vapour saturation pressure mixed with magmatic gas. The initial water composition is that of seawater (Table 5) and the composition of the basaltic glass used for the calculations is given in Table 6. Magmatic gas composition has been simulated based on chemical analyses of volcanic gases emitted in Surtsey, Iceland (Table 7). The secondary minerals considered in the calculations are given in Table 8. In the calculations various proportions of magmatic gas to seawater were mixed followed by dissolution of basalts in series of steps and minerals allowed to precipitate instantaneously upon saturation. The redox state of the solutions in the reaction path calculations was taken to reflect the supply of Fe(II) and Fe(III) from the dissolution reaction and consumption of Fe by secondary minerals. This is a convention most often used for such calculations (e.g. Marini, 2006). However, this may not be the case in open geothermal systems like at Reykjanes with many redox pairs contributing to the overall redox conditions. In addition, it is somewhat uncertain if indeed overall redox equilibrium has been reached in open geothermal systems at temperatures as high as 250-300°C (Stefánsson and Arnórsson, 2002). Because of this, and the simplistic approach used in the reaction path simulations, the results must be viewed with care.

Table 3. Aqueous species included in speciation distribution and mineral saturation state calculations.

Element	Ion, -OH	-Cl	-F	$-SO_4$	-HS	$-CO_2$	-Me
LLNL database							
Si	x		x				x
Na	x	x	x	x		x	x
K	x	x		x			
Ca	x	x	x	x		x	
Mg	x	x	x	x		x	
Fe	x	x	x	x		x	
Al	x		x	x		x	x
CO_2	x						x
H_2S	x						x
SO_4	x						x
Au	x	x			x		
Ag	x	x	x		x	x	
Cu	x	x	x	x	x	x	
Pb	x	x	x	x	x	x	
Zn	x	x	x	x	x	x	
WATEQ database							
Si	x		x				
Na	x		x	x		x	
K	x			x			
Ca	x		x	x		x	
Mg	x		x	x		x	
Fe	x	x	x	x	x	x	
Al	x		x	x			
CO_2	x						x
H_2S	x						x
SO_4	x						x
Au	x	x			x		
Ag	x	x	x	x	x	x	
Cu	x	x	x	x	x	x	
Pb	x	x	x	x	x	x	
Zn	x	x	x	x	x	x	

Table 4. Equilibrium constants as a function of temperature for mineral dissolution and mineral-gas reactions potentially controlling the aquifer fluid composition. The equations are valid at Psat. Unit activity is assumed for all minerals and liquid water.

#	Reaction	logK = a + bT + c/T + dT^2 + elogT					Reference
		a	b	c	d	e	
Mineral reactions							
1	l-alb + $8H_2O$ = Na^+ + $Al(OH)_4^-$ + $3H_4SiO_4$	635.486	0.4057	-16702.0	-2.1245E-04	-283.590	Stefánsson et al. (2009, 2011)
2	mic + $8H_2O$ = K^+ + $Al(OH)_4^-$ + $3H_4SiO_4$	636.075	0.3988	-18302.6	-2.0902E-04	-282.044	Stefánsson et al. (2009, 2011)
3	qtz + $2H_2O$ = H_4SiO_4	-57.702	-0.0106	746.7	-1.5087E-06	22.111	Gunnarsson and Arnórsson (2000)
4	anh = Ca^{2+} + SO_4^{2-}	1804.919	0.8489	-42490.7	-3.8096E-04	-762.156	Stefánsson et al. (2009, 2011)
5	cc + H^+ = Ca^{2+} + HCO_3^-	853.061	0.4131	-18773.4	-1.8914E-04	-361.511	Stefánsson et al. (2009, 2011)
6	chl + $2H_2O$ + $8H^+$ = $5Mg^{2+}$ + $2Al(OH)_4^-$ + $3H_4SiO_4$	340.576	0.4436	11208.0	-2.9070E-04	-190.728	Stefánsson et al. (2009, 2011)
7	czo + $11H_2O$ + H^+ = $2Ca^{2+}$ + $3Al(OH)_4^-$ + $3H_4SiO_4$	1997.556	1.1660	-43989.9	-5.9048E-04	-878.248	Stefánsson et al. (2009, 2011)
8	epi + $11H_2O$ + H^+ = $2Ca^{2+}$ + $Fe(OH)_4^-$ + $2Al(OH)_4^-$ + $3H_4SiO_4$	1224.738	0.7588	-28063.9	-3.9694E-04	-547.838	Stefánsson et al. (2009, 2011)
9	wol + H_2O + $2H^+$ = Ca^{2+} + H_4SiO_4	-91.644	-0.0116	7418.1	-7.9588E-06	34.062	Stefánsson et al. (2009, 2011)
10	pre + $8H_2O$ + $2H^+$ = $2Ca^{2+}$ + $2Al(OH)_4^-$ + $3H_4SiO_4$	1232.731	0.7607	-24606.1	-3.9792E-04	-547.640	Stefánsson et al. (2009, 2011)
11	py + $2H^+$ + H_2(aq) = $2H_2S$(aq) + Fe^{2+}	-169.899	-0.0473	4844.2	1.0275E-05	67.777	Stefánsson et al. (2009, 2011)
12	wai + $10H_2O$ = Ca^{2+} + $2Al(OH)_4^-$ + $4H_4SiO_4$	1219.925	0.7616	-27225.6	-3.9653E-04	-544.465	Stefánsson et al. (2009, 2011)
13	mt + $4H_2O$ = Fe^{2+} + $2Fe(OH)_4^-$	-137.203	-0.0383	101.9	8.9963E-06	46.959	Stefánsson et al. (2009, 2011)
14	gro + $8H_2O$ + $4H^+$ = $3Ca^{2+}$ + $2Al(OH)_4^-$ + $3H_4SiO_4$	1221.164	0.7654	-18849.8	-4.0685E-04	-544.150	Stefánsson et al. (2009, 2011)
15	pyrr + $2H^+$ = Fe^{2+} + H_2S	-283.060	-0.1012	9192.2	3.4229E-05	114.180	Stefánsson et al. (2009, 2011)

Table 4. Cont.

#	Reaction	logK = a + bT + c/T + dT^2 + elogT					Reference
		a	b	c	d	e	
Mineral and gas buffer reactions							
16	1/3 py + 1/3pyrr + 2/3pre +2/3H_2O = 2/3epi + H_2S(aq)	-245.220	-0.1117	2422.3	4.9022E-05	103.976	Stefánsson et al. (2009, 2011)
17	2/3gro + 1/3py + 1/3pyrr + 2/3qtz + 4/3H_2O = 2/3epi + 2/3wol + H_2S(aq)	-243.537	-0.1191	1992.6	5.4405E-05	104.534	Stefánsson et al. (2009, 2011)
18	2gro + 1/4py + 1/2mt + 2qtz + 2H_2O = 2epi + 2wol + H_2S(aq)	93.838	0.0334	-7152.1	-9.6297E-06	-36.000	Stefánsson et al. (2009, 2011)
19	1/4py + 1/2pyrr + H_2O = 1/4mt + H_2S(aq)	-244.317	-0.1128	2702.6	4.9568E-05	103.553	Stefánsson et al. (2009, 2011)
20	6py + 3/2pre + 10H_2O = 2mt + 3/2qtz + czo + anh + 11H_2S(aq)	-5225.473	-2.3344	84692.2	9.7029E-04	2199.004	Stefánsson and Arnórsson (2002)
21	wol + 6py + 11 H_2O = anh + qtz + 2mt + 11H_2S(aq)	-1677.048	-0.6458	5127.4	2.6208E-04	696.705	Supcrt92 Johnson et al. (1992)
22	4/3pyrr + 2/3pre + 2/3H_2O = 2/3epi + 2/3py + H_2(aq)	46.658	0.0123	-2998.3	3.8682E-06	-19.004	Stefánsson et al. (2009, 2011)
23	2/3gro + 4/3pyrr + 2/3qtz + 4/3H_2O = 2/3epi + 2/3wol + 2/3py + H_2(aq)	62.084	0.0157	-3569.7	3.5152E-06	-24.907	Stefánsson et al. (2009, 2011)
24	6gro + 2mt + 6qtz + 4H_2O = 6epi + 6wo + H_2(aq)	160.375	-0.0361	-17219.3	4.6184E-05	-46.378	Stefánsson et al. (2009, 2011)
25	pyrr + H_2O = 3/4py + 1/4mt + H_2(aq)	72.221	0.0164	-3587.8	3.8553E-06	-28.831	Stefánsson et al. (2009, 2011)
26	3/2py + 4.5pre + 8H_2O = 0.5mt + 9/2qtz + 3czo + 3anh + 11H_2(aq)	-3285.059	-1.4852	42034.3	6.6130E-04	1375.829	Stefánsson and Arnórsson (2002)
27	3py + 6wol + 22 H_2O = mt + 6anh + 6qtz + 22H_2(aq)	-6458.827	-2.7165	96711.0	1.1290E-03	2675.646	Supcrt92 Johnson et al. (1992)
28	czo + cc + 3/2qtz + H_2O = 3/2pre + CO_2(aq)	-4.029	0.0034	-1566.5	2.9261E-06	1.146	Stefánsson et al. (2009, 2011)
29	czo + cc+ 3/5qtz = 3/5gro + 1/5H_2O = CO_2(aq)	-66.246	-0.0165	-571.9	9.6457E-06	26.245	Stefánsson et al. (2009, 2011)

l-alb: low-albite, mic: microcline, qtz: quartz, anh: anhydrite, cc: calcite, chl: clinochlore, czo: clinozoisite, epi: epidote, wol: wollastonite, pre: prehnite, py: pyrite, wai: wairakite, mt: magnetite, gro: grossular, pyrr: pyrrhotite

Table 5. Seawater composition after Bruland (1983) unless otherwise specified. Average concentrations at 3.5% salinity.

Element	Probable main species in oxygenated seawater	Conc. µmol/kg
t (°C)		2
pH		7.8
Density (kg/L)		1.023
Salinity		3.50%
Cl	Cl^-	546000
Na	Na^+	468000
Mg	Mg^{2+}	53200
S	SO_4^{2-}, $NaSO_4^-$, $MgSO_4^0$	28200
Ca	Ca^{2+}	10300
K	K^+	10200
C	HCO_3^-, CO_3^{2-}	2300
Br	Br^-	840
B	H_3BO_3	416
Si	H_4SiO_4	100
Sr	Sr^{2+}	90
F	F^-, MgF^+	68
N	NO_3^-, (N_2)	30
Li	Li^+	25
P	HPO_4^{2-}, $NaHPO_4^-$, $MgHPO_4^0$	2.3
Mo	MoO_4^{2-}	0.11
Ba	Ba^{2+}	0.1
As	$HAsO_4^{2-}$	0.023
Al	$Al(OH)_4^-$, $Al(OH)_3^0$	0.02
Ni	Ni^{2+}, $NiCO_3$, $NiCl^+$	0.008
Zn	Zn^{2+}, $ZnOH^+$, $ZnCO_3$, $ZnCl^+$	0.006
Cu	$CuCO_3$, $CuOH^+$, Cu^{2+}	0.004
Cr	CrO_4^{2-}, $NaCrO_4^-$	0.004
Fe	$Fe(OH)_3$	0.001
Mn	Mn^{2+}, $MnCl^+$	0.0005
Au	$AuCl_2^-$	0.000025
Ag	$AgCl_2^-$	0.000025
Co	Co^{2+}, $CoCO_3$, $CoCl^+$	0.00002
Pb	$PbCO_3$, $Pb(CO3)_2^{2-}$, $PbCl^+$	0.00001
O	O_2 (H_20)	0-300
Ti[a]	$Ti(OH)_4^0$	0.021

[a] Li (1982)

Table 6. Basaltic glass composition after Oelkers and Gislason (2001) for major elements and after Peate et al. (2009) for trace elements except for sulphur and carbon.

Major elements (wt %)	
SiO_2	48.12
TiO_2	1.564
Al_2O_3	14.62
Fe_2O_3	1.11
FeO	9.82
MnO	0.191
MgO	9.08
CaO	11.84
Na_2O	1.97
K_2O	0.29
P_2O_5	0.195
Sum	98.8
Trace elements (ppm)	
S	800
Cr	593
V	287
Ni	270
Sr	192
Cu	140
C	120
Zr	94.70
Zn	92
Ba	72.20
Co	59
Sc	39
Y	23.20
Ce	21.77
Ga	16
Nb	14.80
Nd	13.71
La	9.26
Rb	4.80
Dy	3.90
Gd	3.87
Sm	3.56
Pr	3.06
Er	2.29
Yb	2.03
Pb	1.29
Eu	1.26
Lu	0.30

Table 7. Chemical composition of volcanic gases emmited at Surtsey, Iceland (after Sigvaldason and Elísson, 1968). Concentrations are in mol%.

Date of sampling	Sample	H_2O	HCl	SO_2	CO_2	H_2	CO	O_2
1965.02.21	17	86.160	0.400	3.280	4.970	4.740	0.380	0.000
1965.02.21	22	86.160	0.400	1.840	6.470	4.700	0.360	0.000
1965.02.21	24	86.130	0.430	2.860	5.540	4.580	0.390	0.000
Average		86.150	0.410	2.660	5.660	4.673	0.377	0.000
gas/H_2O mol ratio		1.000	0.005	0.031	0.066	0.054	0.004	0.000

Table 8. Secondary minerals observed in the Reykjanes geothermal system and their compositions considered in the present study. Mol fractions calculated based on compositions reported by Marks et al. (2010); Lonker et al. (1993); Freedman et al. (2009).

Secondary mineral	Formula	Mol fraction
Actinolite[1]	$Ca_2(Mg,Fe)_5Si_8O_{22}(OH)_2$	
Tremolite	$Ca_2Mg_5Si_8O_{22}(OH)_2$	1
Albite-low	$NaAlSi_3O_8$	1
Anhydrite	$CaSO_4$	1
Calcite	$CaCO_3$	1
Chalcopyrite	$CuFeS_2$	1
Chlorite[1]	$(Mg,Fe)_5Al_2Si_3O_{10}(OH)_8$	
Clinochlore 7A	$Mg_5Al_2Si_3O_{10}(OH)_8$	1
Chamosite 7A	$Fe_5Al_2Si_3O_{10}(OH)_8$	1
Epidote[1]	$Ca_2FeAl_2Si_3O_{12}(OH)$	
Clinozoisite	$Ca_2Al_3Si_3O_{12}(OH)$	0.24
Epidote	$Ca_2FeAl_2Si_3O_{12}(OH)$	0.76
Galena	PbS	1
Garnet[1]	$Ca_3(Fe,Al)_2Si_3O_{12}$	
Grossular	$Ca_3Al_2Si_3O_{12}$	1
Andradite	$Ca_3Fe_2Si_3O_{12}$	1
Hematite	Fe_2O_3	1
K-feldspar	$KAlSi_3O_8$	1
Magnetite	$FeO \cdot Fe_2O_3$	1
Prehnite[1]	$Ca_2Al(Al,Fe)Si_3O_{10}(OH)_2$	
Al-prehnite	$Ca_2Al_2Si_3O_{10}(OH)_2$	0.82
Pyrite	FeS_2	1
Quartz	SiO_2	1
Sphalerite	(Zn,Fe)S	1
Titanite	$CaTiSiO_5$	1
Wollastonite	$CaSiO_3$	1

[1] solid solution

4 Fluid composition and water-rock equilibria

4.1 Two-phase well discharge and aquifer composition and aqueous speciation

The chemical composition measured in 20 geothermal water and steam samples collected at the surface from the discharge of 8 wells at Reykjanes was used for the reconstruction of the aquifer fluid composition. The row data have been reported by ÍSOR (Iceland GeoSurvey, unpublished data) and by Giroud (2008).

The aquifer composition calculated with the aid of the WATCH program is given in Table 9. The selected reference temperatures used for the calculations were based on downhole measurements and quartz geothermometry temperatures in some cases and ranged from 275°C to 310°C. The obtained pH values in the deep aquifer water were between 4.5 and 5.0. The major components concentrations, in ppm, range as follows: Cl: ~16650-20035; SiO_2: ~580-800; Na: ~8725-10250; K: ~1250-1530; Ca: ~1415-1717; SO_4: ~10-28; CO_2: ~884-2357; H_2S: ~25-90; B: ~5.8-8.8; Fe: ~0.08-3.4; Mg: ~0.5-1.5; Al: ~0.01-0.09; F: ~0.12-0.24; H_2: 0.07-0.6; CH_4: 0.02-0.3 and N_2: 7.8-65.7.

The aqueous speciation distribution of major elements was calculated using two thermodynamic databases, the llnl.dat and wateq4f.dat. The results with respect to the species used for mineral saturation state calculations are given in Appendix A. Interestingly, the predominant species for a given element varies somewhat between the databases (Table 10). In addition, the distribution of redox sensitive components was observed to be different between the databases even though the redox state was fixed in both cases by the H_2S/SO_4 redox pair. In particular, the Fe, Mg and Ca-Cl complexes are apparently more stable according to the llnl.dat database as well as ion-pairs like $NaAl(OH)_4^-$ and $CaSO_4(aq)$. On the other hand, Ca-Cl complexes, which may be important in saline fluids, are not considered in wateq4f.dat, resulting in calculated Ca^{2+} as the dominant species. As discussed below, these variations have important implication for the calculated mineral saturation states in some cases.

In many cases, no high-temperature data exist on ion-pair constants and metal-ligand (Me-ligand) complexes. The values in the databases are, therefore, based on low-temperature values extrapolated to higher temperatures. This explains the difference between the results of the aqueous speciation calculations. In particular, data on Me-CO_2, SO_4, HS and Cl complexes are absent at elevated temperatures and in some cases at all T-p conditions. For example, the $NaHCO_3(aq)$, $MgHCO_3^+$, $CaHCO_3^+$ ion pairs are calculated to be important for CO_2 speciation, accounting for >50% of total dissolved CO_2 under aquifer conditions. However, data on these ion-pair constants only exist at <100°C, and the extrapolated values at 200-300°C for the equilibrium ion-pair constants depend very much on the low-temperature values selected that may vary by >1 log unit.

Table 9. Aquifer water composition at Reykjanes as calculated using the WATCH program. Row data for samples 1-18 are from ISOR (unpublished data) and data for samples 19-20 are from Giroud (2008).

Sample #	Well	$t_{aquifer}$ (°C)	pH	SiO_2 ppm	B ppm	Na ppm	K ppm	Ca ppm	Mg ppm	Al ppm	Fe ppm	Cl ppm	F ppm	CO_2 ppm	H_2S ppm	SO_4 ppm	H_2 ppm	CH_4 ppm	N_2 ppm
1	RN-10	310	4.735	666.13	8.245	9724.26	1496.35	1524.93	1.2	0.0435	3.3634	19126.89	0.212	2352.23	84.81	10.78	0.24	0.32	29.69
2	RN-10	310	4.710	730.71	7.3698	9376.88	1386.93	1480.23	1.082	0.029	2.1404	18432.32	0.204	1986.7	90.11	12.39	0.16	0.11	7.8
3	RN-10	310	4.882	747.79	7.4864	9570.23	1445.51	1538.03	1.222	0.0306	1.9183	18962.21	0.238	1801.1	73.01	10.61	0.27	0.22	30.89
4	RN-10	310	4.814	799.55	7.5957	9441.51	1378.8	1505.54	1.097	0.0145	0.9186	18032.43	0.23	2035.22	87.31	12.42	0.32	0.27	28.41
5	RN-11	295	4.859	678.45	8.0957	9815.14	1436.98	1630.58	0.933	0.0531	0.9856	19359.24	0.229	1778.7	52.89	12.23	0.12	0.21	27.56
6	RN-12	295	4.908	703.9100	7.8349	9670.2700	1417.44	1666.65	0.778	0.0201	0.3673	19237.35	0.219	1700.8	45.5	14.69	0.17	0.12	46.28
7	RN-12	295	4.918	629.09	7.4161	8984.46	1306.91	1515.13	0.62	0.0159	0.3385	17410.72	0.195	1562.61	40.78	16.39	0.1	0.08	30.76
8	RN-12	295	4.951	656.76	7.7902	9403.51	1381.35	1627.63	0.75	0.0312	0.4283	18346.57	0.214	1461.23	38.48	16.51	0.08	0.07	42.49
9	RN-12	295	4.961	664.0000	8.3547	9385.3000	1399.75	1617.58	1.059	0.084	0.1662	18887.84	0.219	1500.69	42.04	17.41	0.08	0.07	15.96
10	RN-12	295	4.983	679.36	8.1007	9495.07	1390.74	1631.71	1.005	0.0596	0.6491	19420.51	0.213	1362.86	24.61	16.01	0.07	0.11	65.7
11	RN-18	285	4.922	602.47	7.771	10194.92	1478.25	1701.77	0.594	0.0545	0.2086	20012.64	0.21	1239.08	34.41	16.94	0.29	0.06	13.93
12	RN-18	285	4.966	626.5	8.165	9962.34	1431.02	1645.84	0.522	0.048	0.3851	19539.53	0.205	901.45	30.95	17.89	0.08	0.03	11.92
13	RN-19	275	4.947	619.31	7.5395	10120.79	1419.03	1507.89	0.592	0.0312	0.0906	19072.97	0.188	1073.39	31.61	19.48	0.26	0.06	12.63
14	RN-19	275	4.970	587.23	8.2213	9965.33	1439.39	1663.69	0.715	0.0477	0.4327	19833.53	0.177	884.42	28.07	23.75	0.11	0.02	9.25
15	RN-19	285	4.956	598.93	7.2913	9787.73	1372.33	1458.26	0.573	0.0302	0.0876	18445.31	0.182	1331.41	38.67	18.84	0.32	0.07	15.75
16	RN-21	284	4.856	621.92	8.77	10178.95	1496.19	1687.7	0.787	0.0771	0.4404	19999.97	0.197	1020.03	35.15	15.93	0.24	0.05	12.71
17	RN-23	305	4.964	701.77	8.3774	10251.14	1529.86	1717.59	1.456	0.0965	2.0965	20035.6	0.219	1301.29	65.2	14.12	0.56	0.13	12.76
18	RN-23	305	4.930	700.73	7.7685	9265.18	1359.93	1503.54	0.839	0.0208	0.8391	18668.78	0.208	1526.91	62	28.55	0.15	0.05	9.49
19	RN-12	285	4.601	616.45	6.1609	9229.52	1301.9	1525.24	0.723	0.0209	0.3918	17511.2	0.117	1906.14	56.59	14.34	0.16	0.09	18.11
20	RN15	276	4.479	581.24	5.8107	8726.38	1251.57	1415.91	0.93	0.0389	0.2534	16650.96	0.119	2357.37	50.35	21.02	0.24	0.15	29.81

Table 10. Dominant species for major components in aquifer fluids according to the LLNL and WATEQ databases.

Element	Dominant species
LLNL database	
Si	H_4SiO_4
Na	Na^+
K	K^+
Ca	$CaCl_2$
Mg	$MgCl^+$
Fe	$FeCl_2^+$, $FeCl_4^{2-}$
Al	$NaAl(OH)_4$
CO_2	CO_2
H_2S	H_2S
SO_4	$CaSO_4$
WATEQ database	
Si	H_4SiO_4
Na	Na^+
K	K^+
Ca	Ca^{2+}
Mg	Mg^{2+}
Fe	$Fe(OH)_3$, Fe^{2+}
Al	$Al(OH)_4^-$
CO_2	CO_2
H_2S	H_2S
SO_4	SO_4^{2-}

In addition, the calculated pH value of the deep liquid inherent large uncertainties. It is based on measured concentrations of weak acids and bases in the surface fluids and conservation of alkalinity and depends on the aqueous species distribution of most major elements in one way or another. For saline waters, the calculation of pH using the WATCH program is subject to substantial error as the complex HCl is not included in the aqueous species. Thus, calculated pH may be up to 0.5 units lower than actual values, this uncertainty is estimated based on dissociational equilibria for HCl at ~300°C. Using conservation of charge balance for pH calculation somewhat different results were obtained for some samples, however, this approach largely depends on the analytical uncertainties of Na and Cl in the saline Reykjanes fluids and resulted in variations between ~4 and ~6.

4.2 Mineral equilibrium

The saturation index of secondary and primary minerals is defined by

$$SI = \log(Q_r/K)$$

where K is the equilibrium solubility constant for a particular mineral dissolution reaction and Q is the reaction quotient given by

$$Q_r = \prod a_i^{v_i}$$

where a_i^v is the activity of the *i-th* mineral or aqueous species and v_i is its reaction stochiometry, positive for products and negative for reactants. For mineral dissolution reactions $Q_r > K$ denotes supersaturation, $Q_r = K$ saturation and $Q_r < K$ undersaturation.

The equilibrium mineral-water reactions potentially controlling the geothermal water composition must involve the observed secondary minerals and in the Reykjanes geothermal system these are among others epidote, prehnite, calcite, anhydrite, clays, zeolites, albite, pyrite, wollastonite, amphibole and quartz (Franzson et al., 2002; Marks et al., 2010). However, as demonstrated by Franzson et al. (2002) the minerals may not have coexisted during the lifetime of the system, and therefore, the fluids of today may not be in equilibrium with all these minerals.

The saturation state with respect to these minerals is shown in Figure 5. The values for the equilibrium solubility constants are given in Table 4 and the secondary mineral activities in Table 8. The reaction quotients, Qr, were calculated both using the llnl.data and wateq4f.dat databases.

Relatively close approach to equilibrium is obtained for most of the minerals, with some systematic differences of importance, for instance, the reaction quotients calculated using the wateq.dat database in general higher than those calculated using the llnl.dat database. The results indicate that difficulties and potential errors associated with the aqueous speciation calculations as well as with elemental analyses are a large source of uncertainties. Low-albite and microcline are calculated to be close to saturation, however, a difference of about 1 log unit was obtained between the databases, largely resulting in differences in the calculated activity of $Al(OH)_4^-$ linked to $NaAl(OH)_4(aq)$ ion-pair constants and Al-OH hydrolysis reactions. In addition, significant scatter is observed in the data points calculated using the same database suggesting analytical problems involved in total Al analysis, which is supported by observation of differences up to ~0.6 orders of magnitude in Al concentrations reported for samples from the same well, but differences in pH also have a significant effect. Similar scatter is observed in the saturation state of other Al-bearing as well as Fe-bearing minerals. Anhydrite and calcite were observed to be supersaturated and undersaturated, respectively, with little scatter but with systematic differences between databases attributed to the calculation of Ca^{2+}. On the other hand, quartz, clinochlore, clinozoisite, epidote, prehnite, pyrite, wairakite, grossular are all observed to be close to saturation and pyrrhotite and wollastonite undersaturated, yet, as mentioned above, large scatter of the data is observed as well as differences between the results of the two databases, except for the case of quartz. For, Fe(III) containing minerals like epidote and magnetite, the calculated reaction quotients using the llnl.dat database were orders of magnitude below saturation (>10 log units). This is due to calculated high stabilities and predominance of Fe(III)-Cl complexes, that is most likely overestimated and inconsistent with magnetite solubility in HCl-NaCl solutions at 200-450°C (Saunier, 2011).

One possible way of decreasing the uncertainties associated with aqueous speciation calculations is to write the reactions of importance in terms of mineral buffers in a way that some aqueous species are cancelled out. Several such mineral buffers have been proposed to potentially control aquifer CO_2, H_2S and H_2 concentration and involve minerals including pyrite, pyrrhotite, prehnite, epidote, clinozoisite, quartz, wollastonite, magnetite, grossular, anhydrite and calcite (Table 4). A reasonable good agreement is observed between the aquifer concentrations of CO_2, H_2 and H_2S and the reactions,

$$czo + cc + 3/2qtz + H_2O = 3/2pre + CO_2(aq)$$
$$3/2pyr + 9/2pre + 8H_2O = 1/2mt + 9/2qtz + 3czo + 3anh + 11H_2(aq)$$
$$6pyr + 3/2pre + 10H_2O = 2mt + 3/2qtz + czo + anh + 11H_2S(aq)$$

assuming $a_{czo} = 0.24$, $a_{pre} = 0.82$ (Lonker et al., 1993; Freedman et al., 2009; Marks et al., 2010) (Figure 6). This is consistent with what was observed by Stefánsson and Arnórsson (2002). Close approach to equilibrium was also observed between H_2 and H_2S concentrations and the reactions,

$$wol + 6py + 11\ H_2O = anh + qtz + 2mt + 11H_2S(aq)$$
$$3py + 6wol + 22\ H_2O = mt + 6anh + 6qtz + 22H_2(aq)$$

which involve only pure minerals, and therefore, avoid uncertainties related to secondary minerals activities in the calculation of the equilibrium constants. Equilibrium curves for buffers involving pyrrhotite plot above the data points, this being consistent with pyrrhotite calculated undersaturated and not reported in alteration mineralogy at Reykjanes. However, unlike for H_2S concentrations, most of the H_2 concentrations plot above the equilibrium curves for the assemblages involving pyrite-prehnite-magnetite-quartz-clinozoisite-anhydrite and pyrite-wollastonite-magnetite-anhydrite-quartz, this trend may be attributed to trace aquifer steam fraction since H_2S is much more soluble than H_2 (Arnórsson et al., 2007). Assuming the former mineral buffer assemblage to control H_2 and H_2S concentrations and using the methodology proposed by Arnórsson et al. (2007), an equilibrium vapor fraction of 0.007 to 0.04 by mass was estimated. However, bearing in mind the uncertainties associated with the calculated equilibrium curves for the mineral buffer reactions, secondary mineral activities, and speciation in saline fluids at high temperatures, it cannot be concluded from the data if indeed such a small steam fraction exists in the Reykjanes system.

Figure 5. Mineral saturation state with respect to (a) low-albite, (b) microcline, (c) quartz (d) anhydrite (e) calcite, (f) clinochlore, (g) clinozoisite, (h) epidote, (i) wollastonite, (j) prehnite, (k) pyrite, (l) wairakite, (m) magnetite, (n) grossular and (o) pyrrhotite. Lines represent equilibrium solubility curves. Data points were calculated using two different databases (llnl.dat and wateq4f.dat). Symbols are the same for all figures.

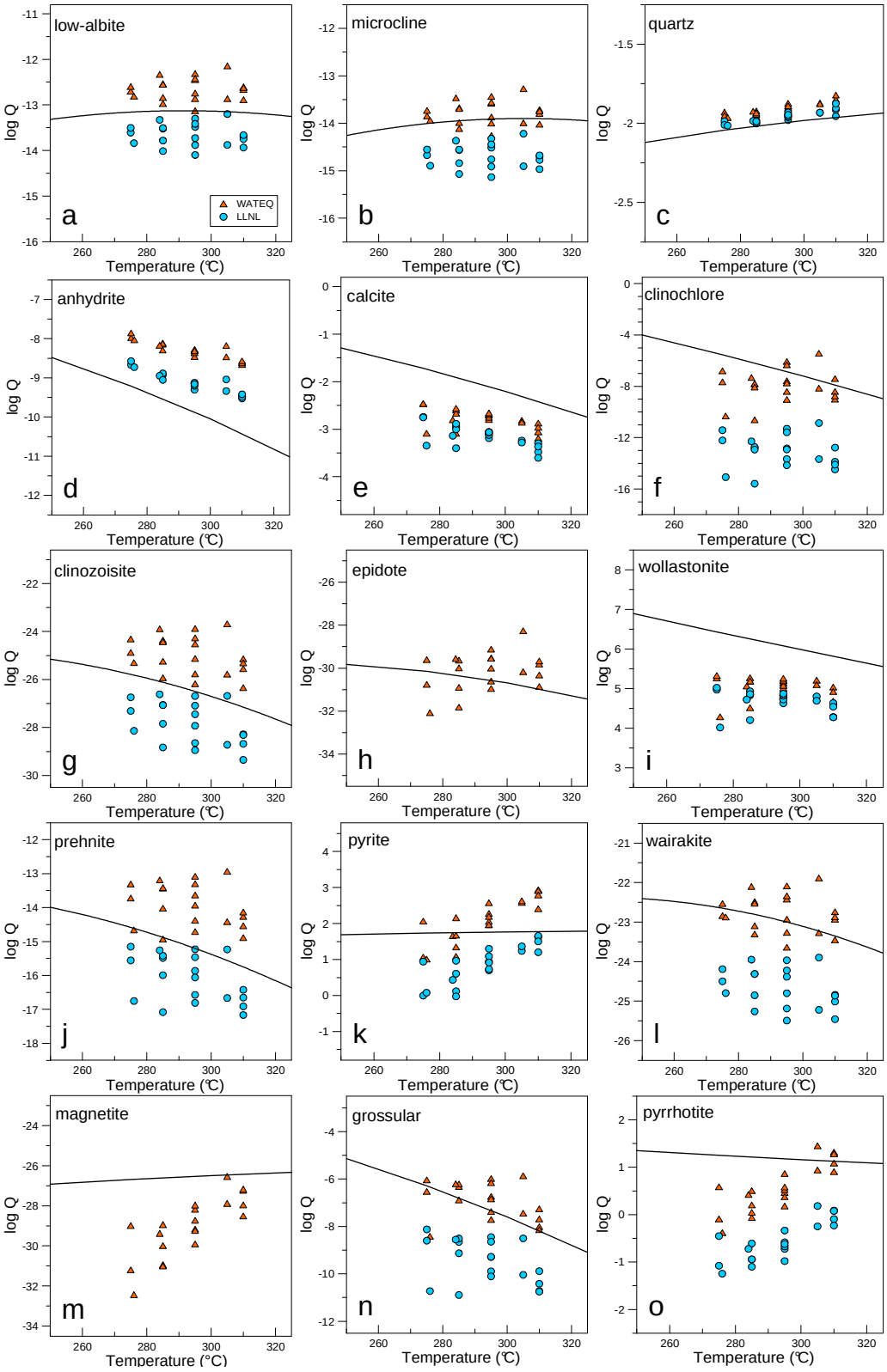

Figure 6. The concentration of (a) CO_2, (b) H_2S and (c) H_2 in aquifer fluids. Lines represent equilibrium constants for mineral-gas reactions (see Table 4) considering average prehnite activity of 0.82 and clinozoisite of 0.24.

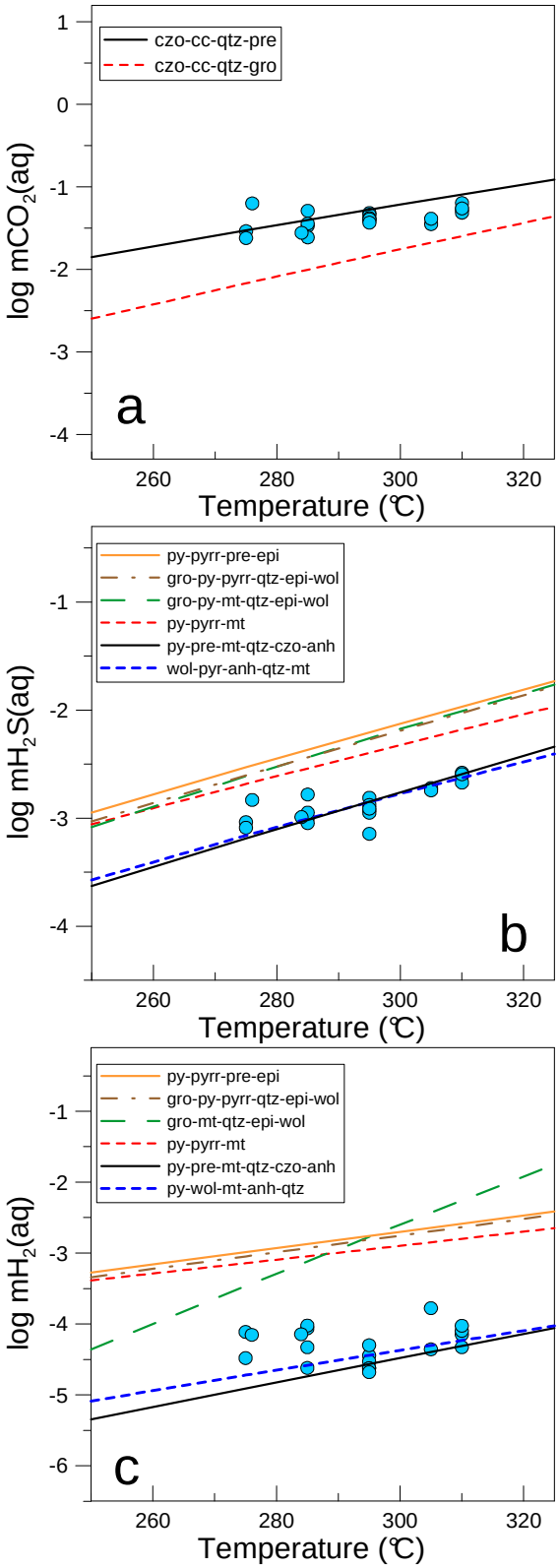

5 Sulphur and carbon transport and precipitation in the Reykjanes geothermal system

5.1 Carbon and sulphur content in altered rocks and secondary mineralogy

For the present study the data on secondary mineralogy and carbon and sulphur abundance were selected from wells RN-10 and RN-17. These wells have been extensively studied for this purpose (Franzson et al., 2002; Wiese et al., 2008; Freedman et al., 2009; Marks et al., 2010) and the present contribution builds on that knowledge. Well number RN-10 is considered to be located within the centre of the present-day thermal anomaly and the highest temperature has been recorded in this well. Well number RN-17 is located approximately 700 m south of the flank of the anomaly and is the deepest well drilled in the Reykjanes geothermal system. The distribution of secondary minerals and measured temperatures in the wells are shown in Figure 7, however, for well RN-17 temperature measurements at depths higher than 2 km were not possible due to the plugging and collapse of the well and they are only estimated. The geothermal wells RN-10 and RN-17 show similar stratigraphic formations and the same alteration zones are consistently observed at approximately similar depths (Freedman et al., 2009).

Pyrite is abundant throughout most of the cuttings intervals in both wells and becomes less abundant below 2000 m depth. Sphalerite is sparsely distributed in well RN-17 from about 400 m to 1200 m, and is found in trace amounts to the base of the well. Chalcopyrite, galena, and other sulphides are also sparsely distributed in RN-17. Anhydrite occurs in trace amounts within the smectite-zeolite zone, epidote-mixed layer clay zone, chlorite-epidote zone and occurs rarely in the epidote-actinolite zone. It is observed from ~200 to ~1500 m in RN-17 and from 100 to 600 m and 1000 to 1400 m depth approximately in RN-10. Calcite is observed in RN-10 from ~1100 m depth up to the surface and from ~350 to ~1100 m as well as from ~2100 to ~2800 m in RN-17. Calcite is not reported in RN-10 below 1100 m (Franzson et al., 2002; Freedman et al., 2009; Marks et al., 2010). Inspections using stereo and petrographic microscopes were performed by Franzson et al. (2002) for mineral identifications in samples from RN-10 whereas backscattered electron imaging was conducted by Marks et al. (2010). The latter method is much more sensitive to small amounts of minerals and, therefore, sulphides like sphalerite, chalcopyrite, and galena probably present in trace amounts in samples from RN-10 may have not been detected.

Total carbon, sulphide, sulphate and total sulphur concentrations were measured in drill cuttings from the wells RN-10 and RN-17 collected at different depths in order to gain insight into the accumulation of these species in the altered rocks and their distribution in the geothermal system. The results are shown in Figure 8. Both total carbon and total sulphur enrichment were measured in the altered rocks compared to reported values of elemental concentrations measured in fresh basalt. This is consistent with previous work (Gunnlaugsson, 1977; Wiese et al., 2008).

Carbon content in the altered rock notably increases as depth decreases from ~0.01 to ~2.0 wt% in the depth range of 1000 to 500 m in well RN-10 and from ~0.01 to ~1 wt% from 1100 to 200 m in RN-17. Below 1100 m, carbon content does not follow a markable trend with respect to depth and values range from < 0.5 ppm to a maximun of ~0.03 wt% in both wells. This is consistent with calcite observed to be more abundant in approximatelly the same depth range in both wells. This may indicate that boiling occurs in the last 1100 m in the geothermal system and this process being responsible for calcite precipitation and increased carbon content in the hydrothermally altered rock. Similar vertical distribution pattern of carbon was reported by Wiese et al. (2008). The very low carbon content in the deepest parts of the wells suggests that carbon mineralization may be not taking place in at least some parts of the aquifer but being leached from rocks.

Sulphide concentrations range from <0.01 to ~1 wt% in well RN-10. The minimun values were obained at ~350, 600, 750 and 850 m and maximum concentrations are observed at 1500 and 150 m depth. In well RN-17 sulphide content ranges from <0.01 (at ~700 and 1150 m) to 1.2 wt%, (at ~150 m). Unlike for carbon content, no markable trend as a function of depth is observed for sulphide concentrations and focussed deposition of sulphide is probably not occurring. Pyrite, the most abundant sulphide mineral is thought to readily precipitate from boiling geothermal waters, in addition, the solubilities of other metallic sulphides may behave in a similar way as for pyrite, however, the observations above indicates that sulphide mineralization mechanism is more complicated than for carbon and is influenced for a set of variables experiencing changes upon boiling and cooling of the fluids.

Measured sulphate concentrations range from ~0.03 to 1.8 wt% at ~800 and 100 m respectively in well RN-10 and from ~0.02 to 0.3 wt% in well RN-17 at ~1600 and 400 m respectively. The highest values were found in the uppermost 400 m depth in both wells. As for sulphide, not a markable trend as a function of depth is observed for sulphate concentrations.

Gunnlaugsson (1977) measured total sulphur in drill cuttings collected at different depths from well number RN-8 at Reykjanes and from wells H3 and H6 in the Krafla and Námafjall geothermal systems, respectively, both associated with dilute fluids. He reported sulphur concentration ranging from 0.1 to 0.55 wt%, from 0.1 to 1.5 wt% and from 0.0 to 6 wt% approximately in the Reykjanes, Námafjall and Krafla systems, respectively, and concluded that vertical distribution pattern of sulphur in Krafla and Námafjall were similar, with sulphur observed to be clearly more abundant in a depth range corresponding to the boiling zone, whereas in Reykjanes sulphur concentrations were observed to be similar at all depths, except for the shallowest part, in Reykjanes. Similar results for sulphur distribution were obtained in this study. These observations suggests that at Reykjanes, sulphur precipitation relatively homogenously as a function of depth may be due to additional sulphur supply from seawater intruding at all depths in addition to sufficient availability of cations, those being mainly metals.

Figure 7. Stratratigraphy, alteration zones, distribution of secondary minerals and isotherms as a function of depth in wells RN-10 and RN-17 (modified from Franzson et al., 2002, Freedman et al., 2009 and Marks et al., 2010).

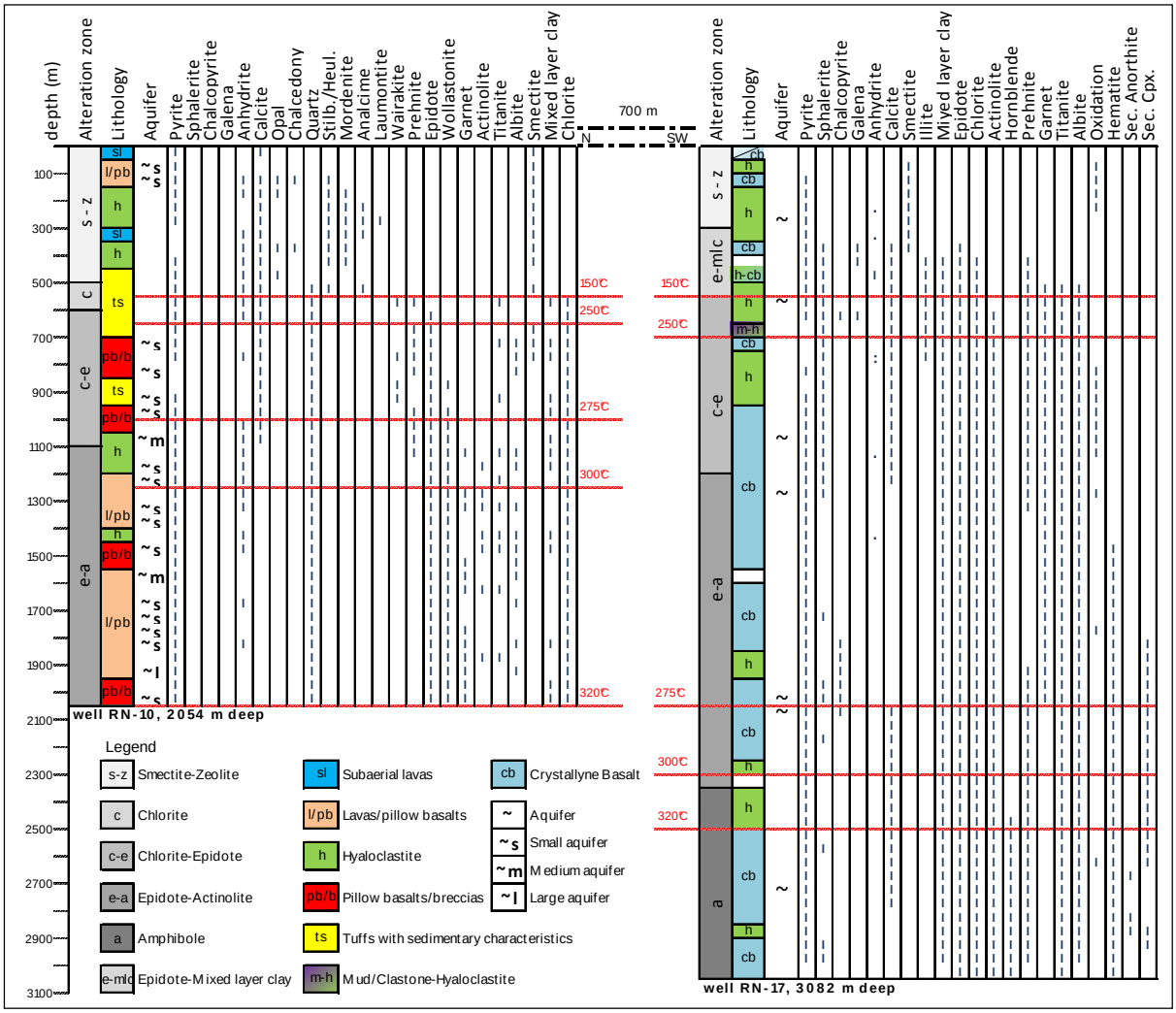

Figure 8. Mass content of (a) total carbon, (b) total sulphur, (c) sulphide, and (d) sulphate measured in drill cuttings from wells number RN-10 and RN-17 as a function of depth. Gray rectangles represent background carbon and sulphur reported by Flower et al. (1982) and Gunnlaugsson (1977), respectively.

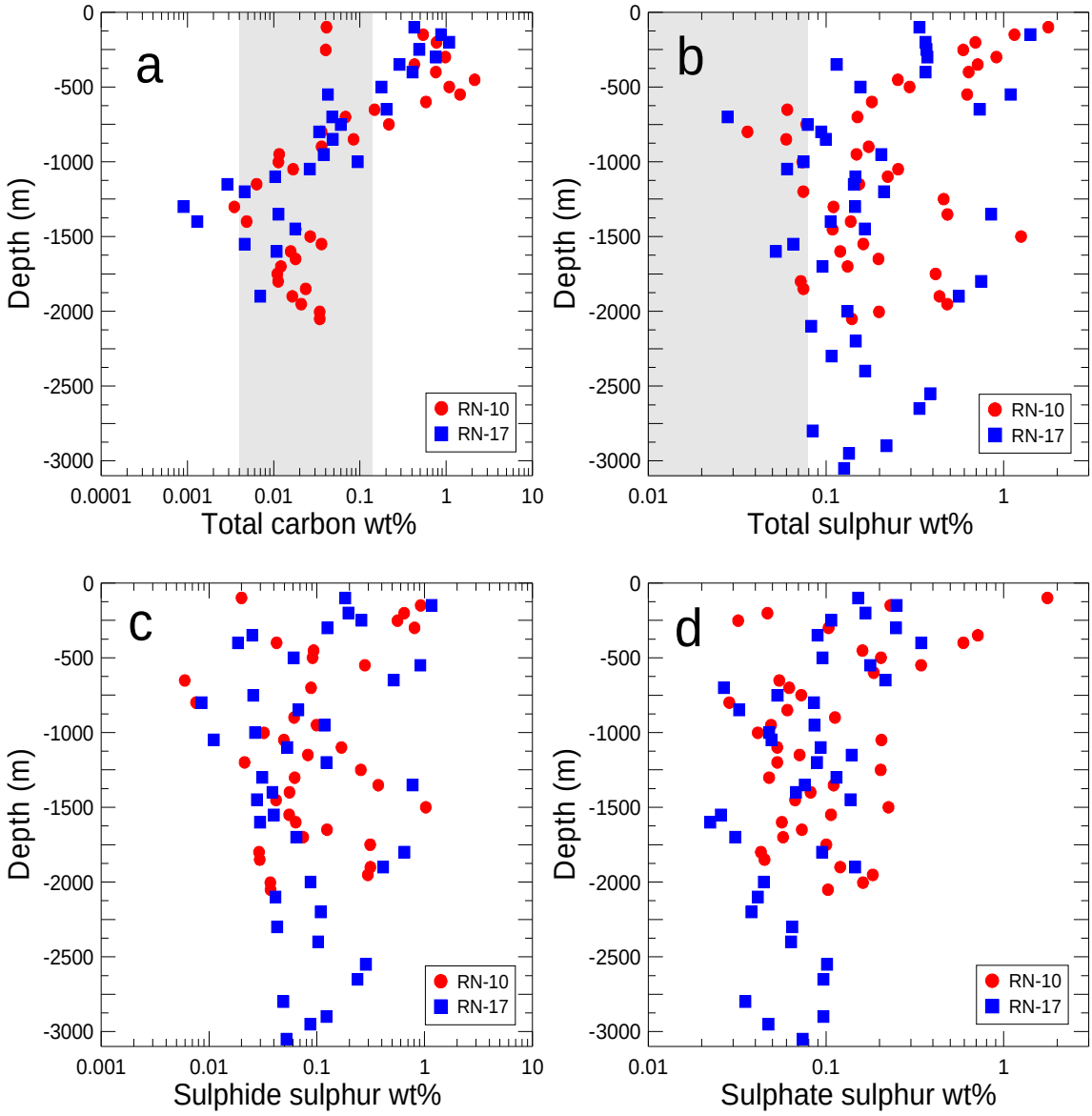

5.2 The transport of H_2S, SO_4 and CO_2 and associated metals in the Reykjanes geothermal system – equilibrium mineral saturation, boiling and cooling

The transport and precipitation of sulphur and carbon in the Reykjanes geothermal system depends on the geochemical behaviour of the components themselves as well as the associated metals known to complex to H_2S, SO_4 and CO_2 and form sulphide, sulphate and carbonate minerals. The most important are various transition metals including Fe, Cu, Zn, Pb and possibly also Ag and Au for sulphide transport and Ca for sulphate and carbonate transport. In addition, redox reactions between H_2S and SO_4 and possibly formation of thermodynamically stable intermediate sulphur species may also be important (Pokrovksi and Dubrovinsky, 2011).

Recent fluid analysis on samples collected downhole at depth between 1350 and 1500 m at Reykjanes (Hardardóttir et al., 2009) have revealed that some of these metals may have been lost upon fluid ascent to the surface (Figure 9). This may be due to quantitative removal of these elements by precipitation. Therefore, in order to study the effects of sulphide, sulphate and carbonate mineral saturation as well as effects of boiling and cooling on their transport and speciation, the aquifer fluid composition was reconstructed based on samples collected at surface from wells RN12, RN-19 and RN-21 for major elements and downhole samples from the same wells for some trace elements (Table 11).

The sulphides pyrite, sphalerite, covellite, acanthite and gold are observed to be supersaturated under aquifer conditions whereas galena is undersaturated (Figure 10). The main sulphate mineral, anhydrite, is also observed to be supersaturated whereas calcite is undersaturated. The saturation state of the sulphide minerals is very dependent on the aqueous speciation calculations and the respective mineral solubilities. For Fe, Cu, Pb, Zn and Ag, free ions, hydroxo and chloro complexes predominated whereas for Au, hydroxo and sulphido complexes were most important. For Ca, SO_4 and CO_2, the Ca^{2+}, $CaSO_4(aq)$ and $CO_2(aq)$ species were most important, respectively, but other species were also present in significant concentrations including $CaCl^+$, SO_4^{2-} and $CaHCO_3^+$.

Upon boiling and cooling, most sulphides became supersaturated or increasingly more supersaturated. This trend suggests that sulphide minerals have the potential to form both upon fluid cooling as well as upon boiling and phase separation. In turns, the saturation to supersaturation of these minerals under aquifer conditions and upon boiling and cooling is somewhat consistent with sulphides being observed relatively homogeneous throughout wells RN-10 and RN-17 (Figure 8) and pyrite and other sulphides present at all depths in the system (Franzson et al., 2002; Freedman et al., 2009; Marks et al., 2010).
The aquifer fluids are calcite undersaturated, the degree of undersaturation was however found to be dependent on both the Ca and CO_2 speciation as well as the pH value. Upon boiling, they become increasingly less undersaturated and in fact supersaturated if uncertainties related to the calculation of pH are considered. Cooling, however, has the reverse trend, making calcite increasingly more undersaturated. These findings are in reasonable agreement with calcite being absent in the deeper parts of the Reykajnes system, whereas upon boiling calcite has the potential to precipitate as observed in increased mass of carbon above 1000 m depth, corresponding approximately to depth of boiling.

Figure 9. Calculated and measured aquifer concentrations of selected (a) major and (b) trace elements at Reykjanes. Calculated concentrations were obtained with the aid of the WATCH program based on surface samples from wells number RN-10, RN-12, RN-15, RN-19, RN-21. Measured compositions in deep liquid samples are from wells number RN-12, RN-19, RN-21, reported by Hardardóttir et al.(2009).

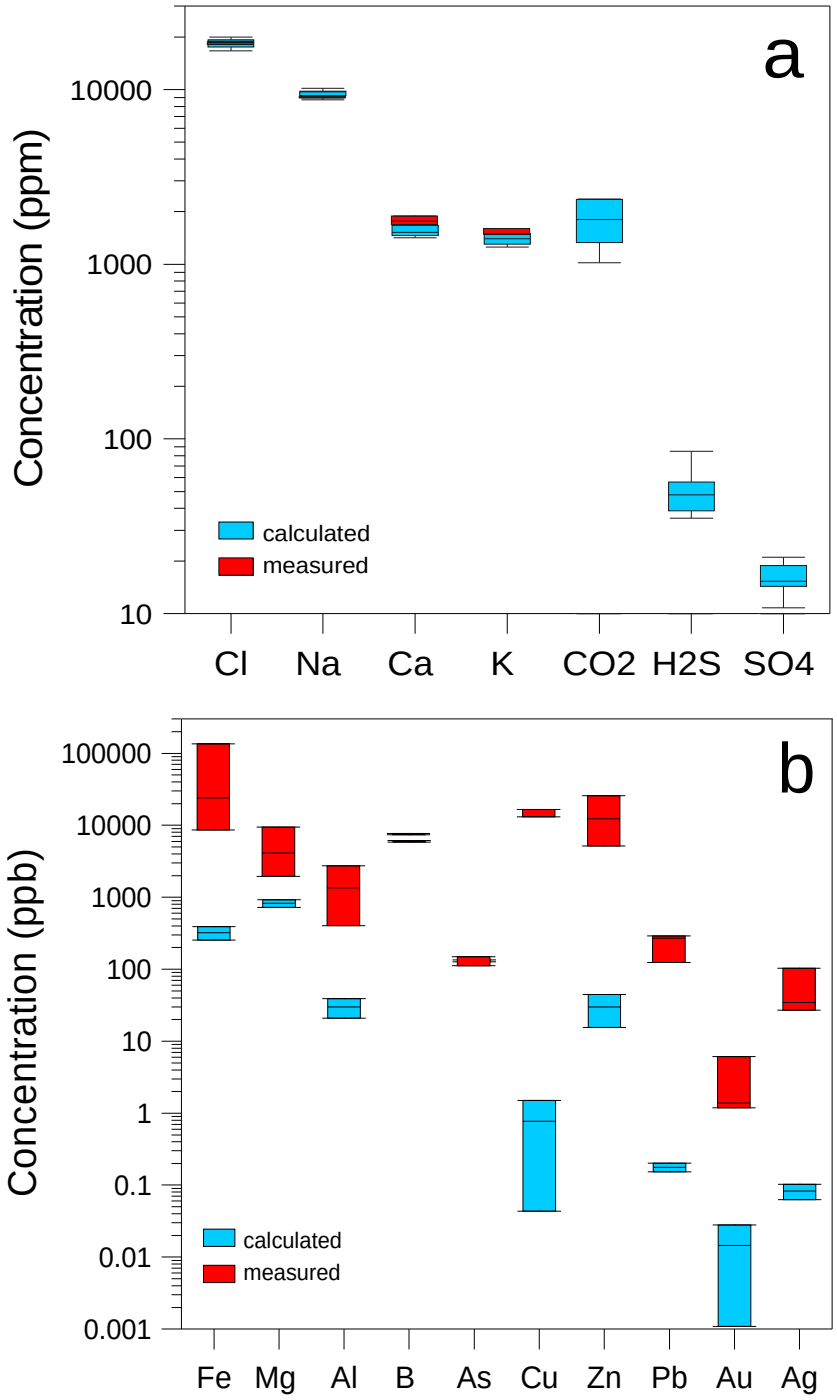

Anhydrite is slightly supersaturated with respect to the aquifer fluids. However, upon both conductive cooling and adiabatic boiling, the fluids become undersaturated. This is in qualitative agreement with anhydrite sporadically being observed in the Reykjanes system (Franzson et al., 2002; Freedman et al., 2009; Marks et al., 2010) and homogeneous sulphate concentrations in the well cuttings as a function of depth but somewhat contradicts the observations of slightly sulphate enrichment in drill cuttings samples from the uppermost 400 m. In addition, it should be kept in mind that the total sulphate and sulphide concentrations in the altered rocks are somewhat higher than in fresh basalts, suggesting that both sulphides and sulphates have potentially formed in the Reykjanes geothermal. Sulphate mineralisation may occur not only as an effect of boiling and cooling of ascending geothermal waters but also as a result of mixing of rising steam with colder seawater in the shallowest part of the system, this leading to anhydrite precipitation from the heated seawater due to its retrograde solubility.

Table 11. Aquifer fluid composition at Reykjanes based on surface and downhole samples for major and trace elements, respectively.

Well #	RN-12	RN-19	RN-21
$t^{aquifer}$ (°C)	295	275	284
pH	4.94	4.96	4.86
Major elements, mmol/kg [a]			
SiO_2	11.09	10.02	10.35
B	0.731	0.711	0.811
Na	408	433	443
K	35.27	36.07	38.27
Ca	40.21	38.50	42.11
Mg	0.035	0.026	0.032
Cl	526	539	564
F	0.0112	0.0096	0.0104
CO_2	34.49	24.91	23.18
H_2S	1.12	0.96	1.03
SO_4	0.17	0.22	0.17
H_2	0.050	0.114	0.119
CH_4	0.0056	0.0031	0.0031
Trace elements, µmol/kg [b]			
Fe	430	154	2431
Al	101	15	50
Cu	261	208	207
Ag	321	250	960
Au	31	6	7
Zn	393	79	189
Pb	1.3	0.6	1.4

[a] Based on data given in Table 10

[b] Hardardóttir er at. (2009)

Figure 10. The mineral saturation state at aquifer conditions and upon adiabatic boiling and conductive cooling for phases of importance for H_2S, SO_4 and CO_2 transport. The solid lines show the boiling trends and the dashed lines the cooling trends. Calculations based on samples from wells RN-12, RN-19 and RN-21 and using the llnl.dat database.

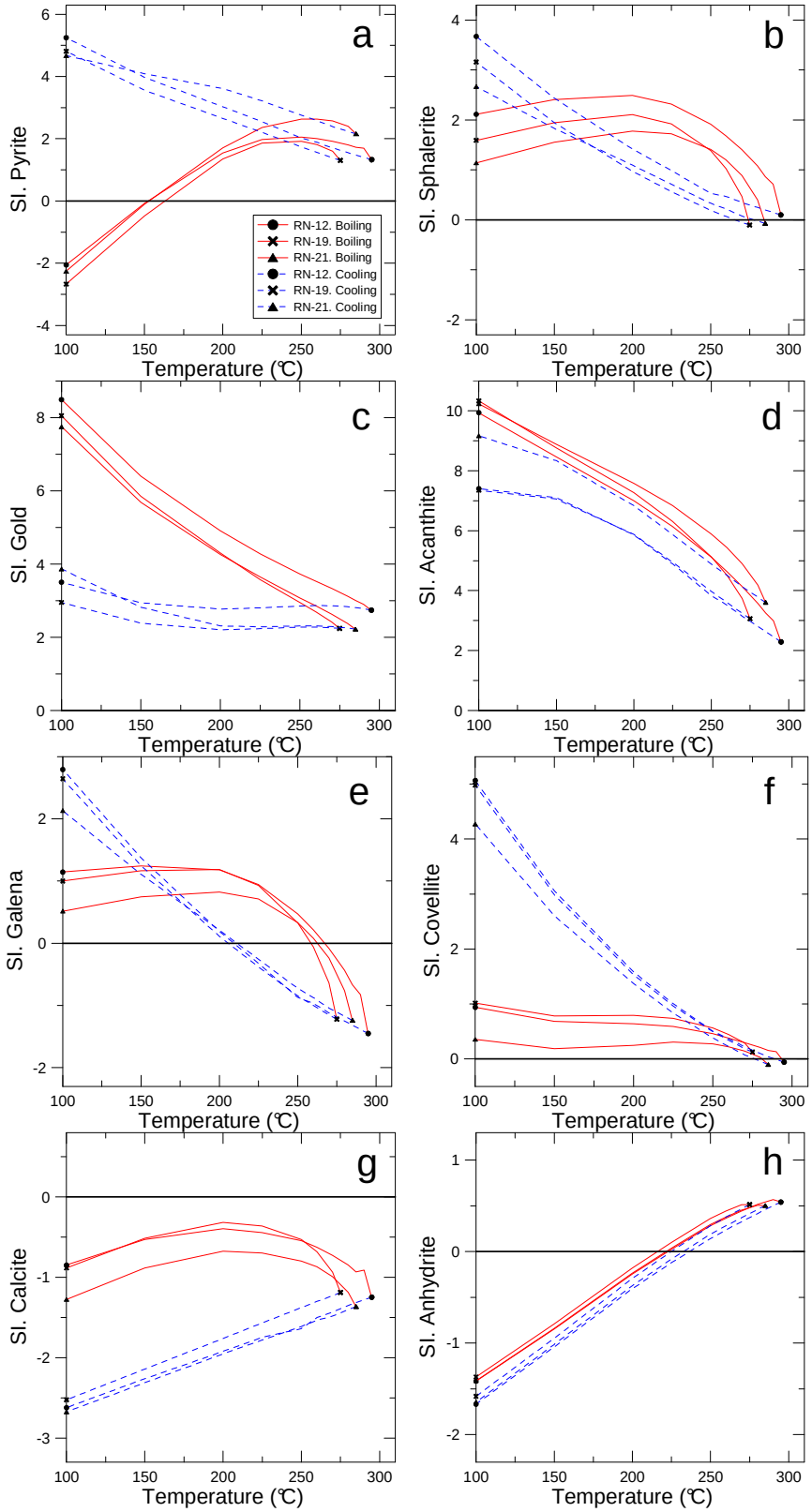

To better constrain the effects of mass movement of sulphur and carbon upon cooling and boiling a series of model calculations were conducted using both the WATCH and PHREEQC programs and the llnl.dat database with the latter program. The initial aquifer fluids were assumed to be saturated with given sulphides including pyrite, sphalerite, galena, covellite and acanthite, as well as calcite and anhydrite. Upon supersaturation, the excess minerals were allowed to precipitate simultaneously and the resulting solution composition calculated. The elemental ratios between the boiled and cooled waters without precipitation on one hand and with mass precipitation on the other were then calculated. The difference is taken to indicate mass loss of H_2S, SO_4 and CO_2 from solution upon boiling and cooling. The results are shown in Figure 11. As shown, sulphide seems to be quantitatively removed from solution upon boiling and to less degree upon fluid cooling mostly into pyrite but also sphalerite, galena and covellite. Sulphate, on the other hand seems to be unaffected by cooling whereas small fraction (<20%) may be lost upon boiling. For CO_2, the results are similar to those of SO_4, suggesting that most CO_2 and Ca by mass are transported from the aquifer to the surface, this being consistent with similar surface and down-hole concentrations of Ca (Hardardóttir et al., 2009). However, upon continuous boiling, calcite may build up in the altered rocks above background (rock) concentrations as observed (Figure 8).

5.3 Carbon and sulphur mass of precipitation

Based on measured concentrations of total carbon, total sulphur, sulphide and sulphate in drill cuttings samples, the mass of mineralization of each species was calculated. These masses were estimated separately for three vertical sections in the system, i.e. depth ranges, considering that the rate of mineralization may be a function of the depth at which the transporting fluids are encountered. The vertical sections considered are: from the surface to 1100 m (section 1, regarded as the zone of extensive boiling), from 1100 to 2000 m (section 2) and from 2000 to 3000 m (section 3).

Considering carbon content in fresh basalt of 0.012 wt% and sulphur content of 0.08 wt% (Gunnlaugsson, 1977; Flower et al., 1982) and subtracting these amounts from measured concentrations, the average elemental enrichment in altered rocks were calculated as follows, carbon: ~0.353 wt% in the upper 1100 m and no enrichment in the deeper parts; sulphur: ~0.305, 0.197 and 0.099 wt% in section 1, section 2 and section 3 respectively. In addition, a minimum enrichment of sulphide and sulphate was calculated assuming that background sulphur of 0.08 wt% would account for only sulphide or only sulphate. Accordingly, sulphide enrichment is calculated to be: ~0.119, 0.105 and 0.033 wt% in sections 1, 2 and 3, respectively; and for sulphate: 0.106% in the upper 1100 m and no enrichment in the deeper parts.

Pálmason et al. (1985) estimated the extent of the Reykjanes geothermal system to be about 2 km^2. Assuming an average density of basaltic host rocks of 2700 kg/m^3 and taking carbon and sulphur concentrations in wells RN-10 and RN-17 to be representative, the total mass of mineralization in the geothermal system, 3 km deep, was calculated. The mass of carbon precipitated in the upper 1100 m as a result of geothermal alteration is approximately 21.1 Mt, sulphur mineralization accounts for 33.1 Mt, sulphide for 14.0 and sulphate for 6.3 Mt. It is worth noting that the result of adding up together the mass of mineralization of sulphide and sulphate does not correspond to mass of mineralization of total sulphur since, as mentioned above, calculated numbers for sulphide and sulphate are based on minimum enrichment, i.e. background sulphur of 0.08 wt% was subtracted from measured concentrations in altered rocks for both sulphur species.Weise et al., reported 14

Mt of carbon (corresponding to 56 Mt of CO_2) fixed in rocks at Reykjanes considering a higher value, 0.02 wt%, for background carbon compared to this study.

The Reykjanes geothermal system has been estimated to be active in the last 18000 to 20000 years based on observations on recent eruptions in the area (Franzson et al., 2002; Hardardóttir et al., 2009; Pope et al., 2009). Taking 20000 years as the life time of the system the average elemental mass of mineralization are calculated as follows, total sulphur: 1653 tonne/yr, sulphide: 700 tonne/yr, sulphate: 315 tonne/yr and carbon: 1054 over the life time of the system.

Figure 11. The effects of adiabatic boiling (solid lines) and conductive cooling (dotted lines) on (a) H_2S, (b) SO_4 and (c) CO_2 loss from solution assuming aquifer fluids initially saturated with selected minerals, those included in Figure 10.

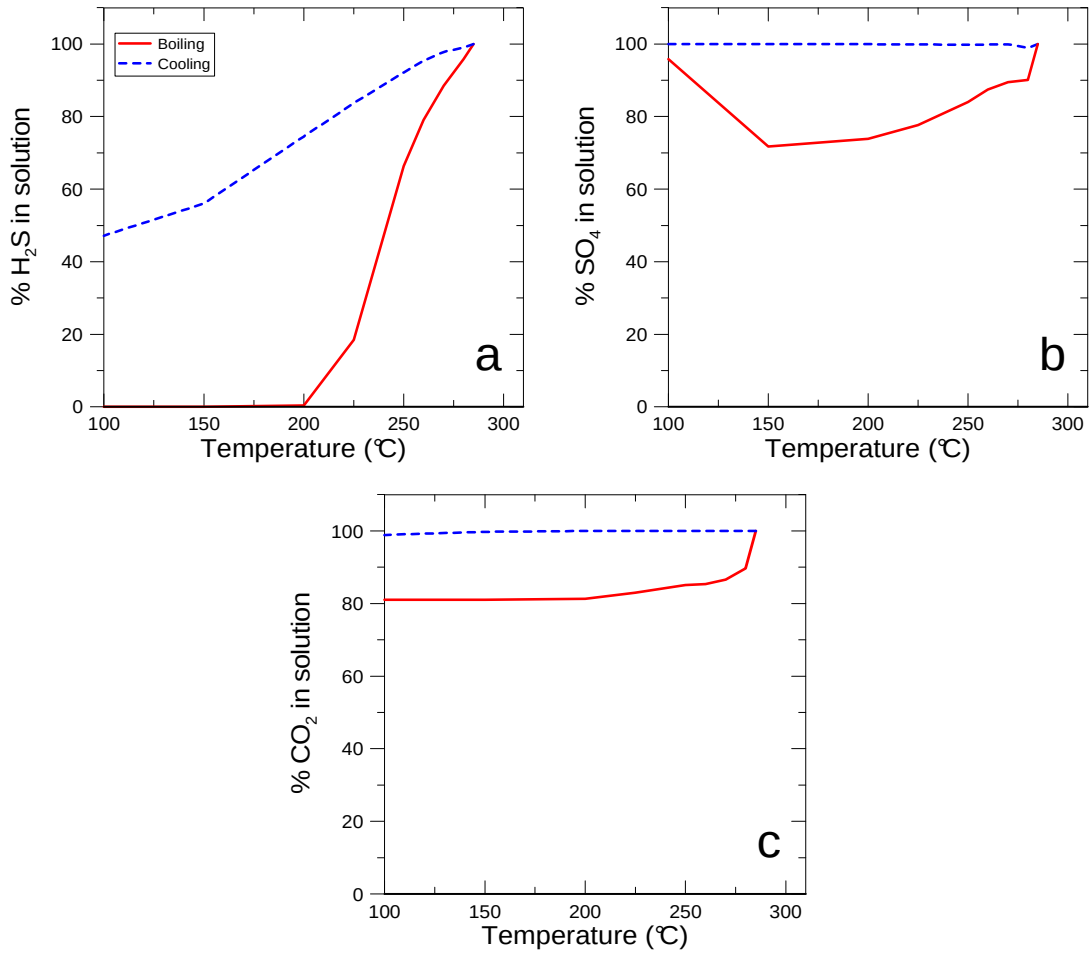

6 Gas-water-rock interaction and source of carbon and sulphur in the Reykjanes geothermal system – reaction path modelling

From the results on carbon and sulphur concentrations in well cuttings it is apparent that these elements build up in the system above background basalt concentrations. One possible source of the elements is magma degassing CO_2 and SO_2 among other gases into the geothermal fluids. Fluid-rock interaction may also contribute. To get insight into this gas-water-rock interaction, reaction path modelling calculations using the PHREEQC program and the llnl.dat database were conducted. The initial reactants include seawater, basalt and volcanic gases (Tables 5-7) and secondary minerals potentially formed are shown in Table 8. The main variables considered in the calculations were magmatic gas supply and extent of reaction. These variables may be interrelated and affect each other e.g. higher gas supply (acid) requires more primary minerals (base) to react with to reach a given conditions. It should be clear that changes in the variables mentioned above lead to variations in other parameters potentially playing a significant role in the chemistry of the system, including the carbon, sulphide and sulphate aqueous concentrations, transport and mineralization. These parameters include pH, oxidation state and mobility of cations.

The results of the model calculations are shown in Figures 12-15. Secondary minerals formed are dependent on the extent of reaction as well as magmatic gas supply (Figure 12). Calcite formation is not observed at 300°C and 0.1 to 5 wt% of magmatic water per 1 kg of seawater, this is consistent with calcite being undersaturated with respect to the fluids. If this is the case is somewhat uncertain as the results are very dependent on aqueous speciation and particularly pH. Carbonate mineralization may be suppressed by mass at aquifer conditions as Ca^{2+}, Fe^{2+}, Mg^{2+} may be predominantly taken up by other secondary minerals including epidote, prehnite, and chlorite. The availability of these cations seems to be controlled by mineral equilibria and being relatively insensitive to acid supply (Figure 13). Increased gas supply does not result in calcite precipitation at aquifer temperature. Anhydrite is observed to form at low reaction progress, but disappears as the fluid-rock reaction proceeds. In addition, hematite is replaced by magnetite at certain extent of reaction. This occurs as the fluid becomes more reduced as reaction proceeds due to supply of Fe^{2+} from the basalts to the waters. Pyrite and chalcopyrite precipitate over the whole extent of reaction; sphalerite appears at certain water-rock ratio. Increased gas supply results in slightly increased rate of sulphide and sulphate mineralization.

Increased gas supply results in initially decreased pH of the solution, nevertheless, at certain extent of reaction (water-rock ratio) the pH seems to reach a balance between basalt dissolution, precipitation of secondary minerals and weak acid ionisation (Figure 14). It can be seen from the figure that for gas supply of 0.1 to 1 wt% the pH is about constant in a wide range of water-rock ratio (from ~90 to ~210 grams of basalt reacted with 1 kg of seawater) corresponding to a steady state in the system where specific mineral assemblages are stable. Higher gas supply requires more mass of rock reacted to attain this state, yet, the

trends of the curves representing different amounts of gas added to the system are very similar.

Figure 12. The effect of magmatic gas supply on secondary mineral formation at 300°C.

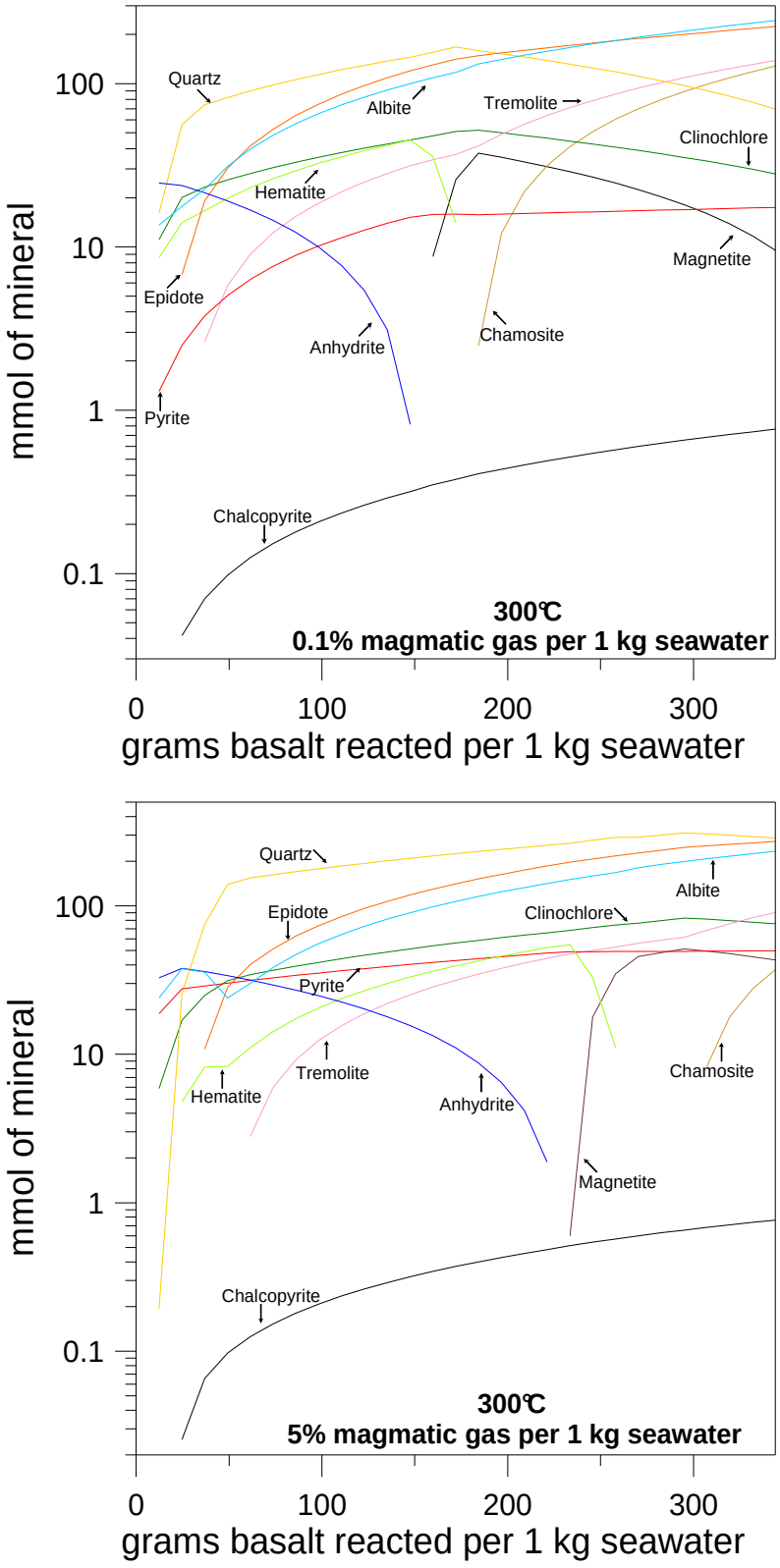

Figure 13. The effect of magmatic gas supply on (a) Ca^{2+}, (b) Fe^{2+} and (c) Mg^{2+} activity during fluid-rock interaction at 300°C.

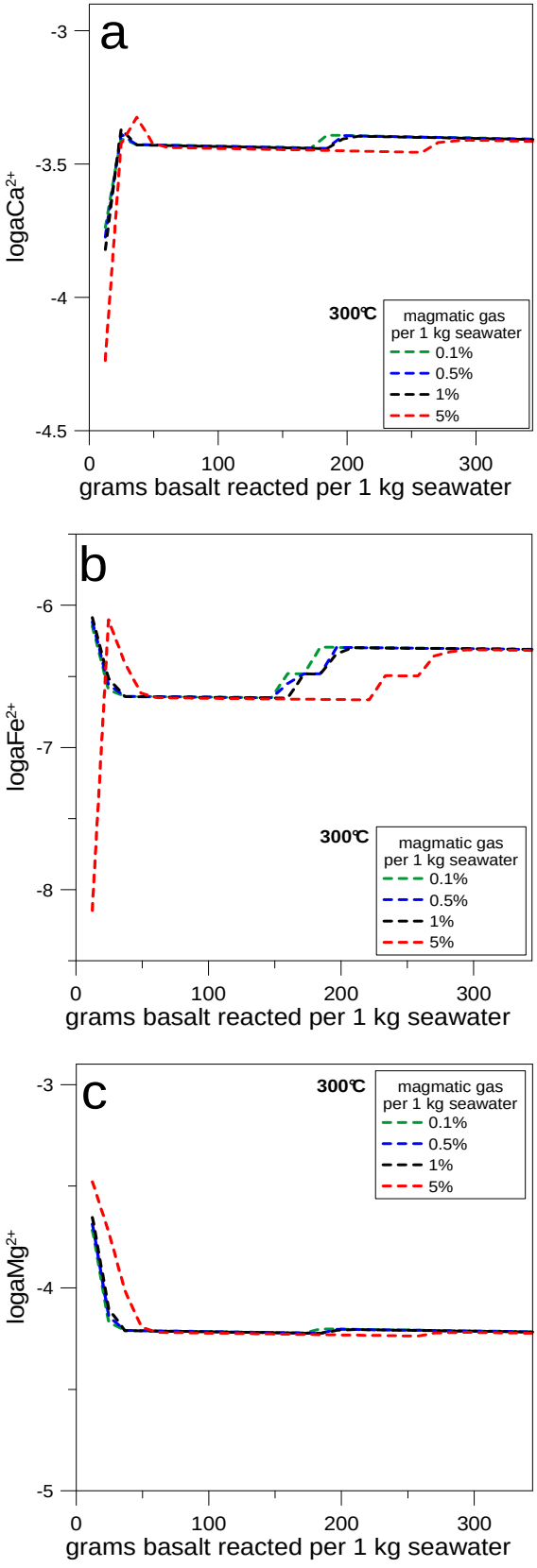

Dissolved H_2S and SO_4 are initially increased by gas supply but upon reaction progress they become buffered by mineral buffer reactions values corresponding to closely to present-day aquifer compositions (Figure 15). As basalt dissolution proceeds, the system moves toward more reduced conditions. These results in anhydrite dissolution and supply of SO_4 that is instantaneously reduced to H_2S suggesting that the distribution of sulphur species and oxidation state may be influenced by the extent of reaction. On the other hand, the aquifer CO_2 concentrations were calculated to depend on magmatic gas supply. This is considered to be caused by limitation of the availability of cations including Ca^{2+}, Mg^{2+} and Fe^{2+} that were predominantly mineralized into minerals including epidote, chlorite, anhydrite, pyrite and iron oxides, in addition to the effects of high temperature and low pH at aquifer conditions resulting in calcite undersaturation. If this is truly the case, it raises the question if indeed CO_2 aquifer concentrations are truly controlled and buffered (Figure 6) or dominated by the supply of magma gases to the geothermal convection cell. At high extent of reaction, CO_2 concentration was observed to slightly decrease, particularly at 5% of gas to seawater ratio. This is due to reduction of carbonate and formation of methane as the system becomes more reduced with reaction progress. This is not likely to occur in the natural system but a modelling limitation since the simulation considers only an initial gas input and not constant supply, i.e. open system, as occurs in nature.

The results of the gas-water-rock reaction modelling suggest that the aquifer fluids are produced upon mixing between very small amount of magmatic gas containing among others CO_2 and SO_2 followed by interaction with the host rocks. The exact proportions are somewhat unclear, but are probably in the range 0.1-1% by mass magmatic gas consistent with previous work (Arnórsson, 1995). However, large uncertainties are associated with these calculations related to aqueous speciation and mineral stabilities and the results needs to be viewed with care. Nevertheless, the point towards the conclusion that the fluid composition including pH, H_2S, SO_4 is somewhat insensitive to small variations in magma gas supply whereas CO_2 concentration is more influenced by the inflow of magmatic gas to the system. This somewhat contradicts to the result of CO_2 being controlled by a mineral-buffer reaction, however, the absence of calcite under aquifer conditions is in line with calcite observed to be slightly undersaturated (Figure 5).

Figure 14. The effect of magmatic gas supply on pH. Gray rectangle represents approximately present-day aquifer values.

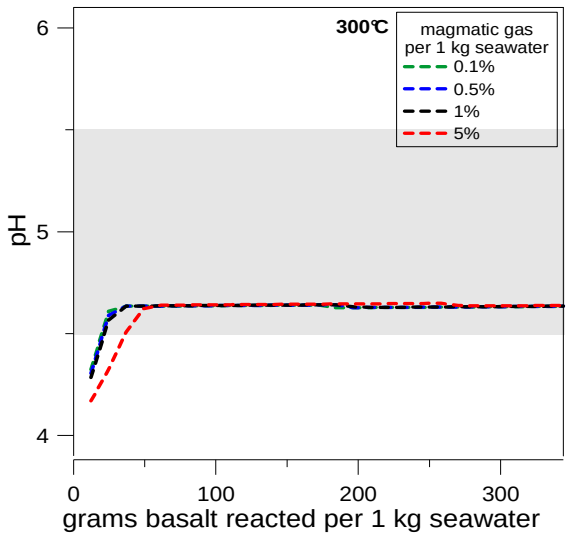

Figure 15. The effect of magmatic gas supply on (a) H_2S, (b) SO_4 and (c) CO_2 concentrations of the resulting solution during fluid-rock interaction at 300°C. Gray rectangles represent present-day aquifer values.

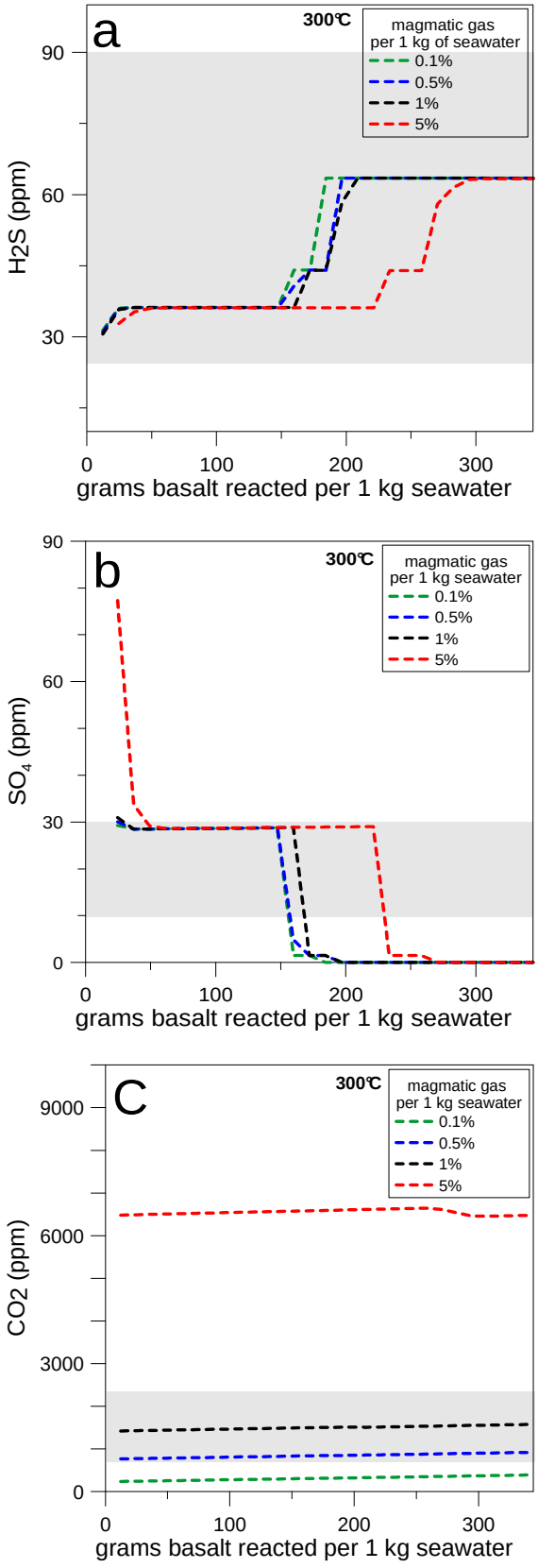

7 Summary and conclusions

Carbon and sulphur are among the major components in geothermal fluids. The transport and precipitation of sulphur and carbon in the Reykjanes geothermal system is influenced by the geochemistry of associated metals known to complex to H_2S, SO_4 and CO_2 and the formation of sulphide, sulphate and carbonate minerals. The most important metals are Fe, Cu, Zn, Pb and possibly also Ag and Au for sulphide transport and Ca for sulphate and carbonate transport. Recent fluid analysis on samples collected downhole at Reykjanes revealed that some of these metals may have been lost upon fluid ascent to the surface most likely due to precipitation (Hardardóttir et al., 2009). In addition, scales enriched in metals, are commonly observed in pipelines at Reykjanes (Hardardóttir et al., 2010). In order to get insight into the source, transport and precipitation of sulphur and carbon in the Reykjanes geothermal system and the associated metal transport and precipitation, the effects of various processes including boiling and phase separation and cooling in addition to gas-water-rock interaction and magmatic input were assessed using data on fluid discharge, deep liquid composition and mass of sulphur and carbon precipitation as well as various types of geochemical modelling.

The measured aquifer temperatures at Reykjanes range from 275 to 310°C and the estimated pH from ~4.5 to ~5.0, however, actual pH values in the aquifer may be up to 0.5 pH units higher. Aquifer fluids at Reykjanes seems to be the formed by mixing of seawater with very small amount of magmatic gas followed by interaction with basaltic host rocks, resulting in geothermal water enriched in SiO_2, K, Ca and depleted in SO_4 and Mg but with Cl concentration close to that of seawater.

Relatively close approach to equilibrium was obtained for most of the minerals including low-albite, microcline, clinochlore, clinozoisite, epidote, prehnite, pyrite, wairakite, grossular. Anhydrite was observed to be supersaturated and calcite, wollastonite, magnetite and pyrrhotite undersaturated. A reasonable good agreement is observed between the aquifer concentrations of CO_2 and the mineral assemblage clinozoisite-calcite-quartz-prehnite, and the H_2 and H_2S concentrations are close to equilibrium with the buffers pyrite-prehnite-magnetite-quartz-clinozoisite-anhydrite and pyrite-wollastonite-magnetite-anhydrite-quartz, particularly when average reported mol fractions for prehnite of 0.82 and 0.24 for clinozoisite are taken into account (Lonker et al., 1993; Freedman et al., 2009; Marks et al., 2010). Some of the H_2 concentrations plot above the equilibrium curves for both mineral buffers, possibly due to trace aquifer steam fraction. Equilibrium steam fraction was calculated to range from 0.007 to 0.04 by mass assuming pyrite-prehnite-magnetite-quartz-clinozoisite-anhydrite to control H_2 and H_2S concentrations in the aquifer fluids. However, considering the uncertainties associated with the calculated equilibrium curves for the mineral buffer reactions and secondary mineral activities, it cannot be concluded if indeed a small steam fraction exists in the Reykjanes system. Important systematic differences exist in the minerals saturation states calculated using two databases related to the aqueous species considered.

Based on reaction path modelling, H_2S and SO_4 aquifer concentrations, in addition to pH, are buffered by fluid-rock interaction whereas CO_2 concentration was observed to be more sensitive to the supply of magmatic gas to the system. This is considered to be caused by limited availability of cations including Ca^{2+}, Mg^{2+} and Fe^{2+} that were predominantly mineralized into epidote, chlorite, anhydrite, pyrite and iron oxides and

resulting in calcite undersaturation. If this is truly the case, it raises the question if indeed CO_2 aquifer concentrations are controlled by mineral buffers or dominated by the supply of magma gases to the geothermal convection cell.

Both carbon and sulphur enrichment were measured in the altered rocks compared to concentrations in unaltered basalt. Carbon content notably increases as depth decreses from ~0.01 to ~2.0 wt% in the depth range of 1000 to 500 m in well RN-10 and from ~0.01 to ~1 wt% from 1100 to 200 m in RN-17. Below 1100 m, carbon content does not follow a markable trend with respect to depth and values range from <0.5 ppm to a maximun of ~0.03 wt% in both wells. These results, are consistent with previous observations on vertical distribution patterns of carbon and with calcite being more abundant in approximatelly the same depth range in both wells. Modelling calculations revealed that aquifer fluids are probably calcite undersaturated and precipitation was not observed at 300°C and 0.1 to 5 wt% of magmatic water per 1 kg of seawater. Upon boiling and phase separation the fluids become increasingly less calcite undersaturated and even supersaturated if uncertainties related to pH calculation are considered. Cooling, on the other hand, makes calcite increasingly more undersaturated. These findings suggest that at aquifer conditions carbon mineralization is probably not taking place. Upon boiling, calcite precipitates and builds up in the altered rocks above background carbon above 1100 m depth, corresponding approximately to depth of boiling.

Sulphide concentrations range from <0.01 to ~1.2 wt% in wells RN-10 and RN-17. Unlike for carbon, no markable trend as a function of depth is observed for sulphide concentrations and focussed deposition of sulphide is probably not occurring. The reconstruction of aquifer fluid composition based on surface fluids analyses for major components and measured metals concentrations in deep liquid and geochemical modelling calculations indicate that most sulphides including pyrite, sphalerite, covellite, acanthite and gold are supersaturated under aquifer conditions whereas galena is undersaturated. Upon boiling and cooling the sulphides become increasingly more supersaturated and saturated for the case of galena. This suggests that sulphide minerals have the potential to form both at aquifer conditions and upon fluid cooling. In addition, sulphide seems to be quantitatively removed from solution upon boiling and to less degree upon fluid cooling mostly into pyrite but also sphalerite, galena and covellite when these minerals are assumed to be initially saturated and allowed to precipitate. These findings support to a certain extent the observation of sulphide precipitation being relatively homogeneous throughout wells RN-10 and RN-17 and pyrite and other sulphides present at all depths in the system. However, either the metals precipitating mainly as sulphides are quantitatively removed from solution during ascent to the surface of geothermal fluids is not known.

Measured sulphate concentrations range from ~0.02 to 1.8 wt% in wells RN-10 and RN-17. The highest values were observed in the range of 100 to 400 m depth in both wells and no markable trend as a function of depth below 400 m. Anhydrite was calculated to be slightly supersaturated with respect to the aquifer fluids and upon both conductive cooling and adiabatic boiling the fluids become undersaturated. Furthermore, sulphate seems to be unaffected by cooling whereas only <20% may be lost from solution upon boiling. These observations somewhat contradicts homogeneous sulphate concentrations measured in the well cuttings as a function of depth, higher than in fresh basalt with preferential enrichment in the uppermost 400 m and anhydrite observed in trace amounts at all depths but rarely in the deepest part of the system. The findings suggest that sulphate mineralisation occurs not only as an effect of boiling and cooling of ascending geothermal waters but mainly as a result of mixing of rising steam with colder seawater in the shallowest part of the system.

Total sulphur vertical distribution pattern in the Reykjanes geothermal system differs to sulphur distribution in other geothermal systems in Iceland associated with dilute geothermal fluids where preferential precipitation is observed in the boiling zones as is the case for carbon in the Reykjanes system. The possible causes for this observations are either significant sulphides precipitation occurring at all depths due to actual metals concentrations in the aquifer much higher than measured at the surface or enhanced sulphur precipitation both as sulphides and sulphates due to additional sulphur supply from seawater intruding at all depths, or both.

Based on measured elemental content carbon enrichment in altered rocks of ~0.353 wt% in the upper 1100 m and no enrichment in the deeper parts was calculated. The minimum enrichment of sulphides was calculated to be ~0.119, 0.105 and 0.033 wt% in the vertical sections from the surface to 1100 m (boiling zone), from 1100 to 2000 m and from 2000 to 3000 m, respectively. Sulphur enrichment is ~0.305, 0.197 and 0.099 wt% in the same vertical sections and minimum sulphate enrichment is ~0.106% in the upper 1100 m and no enrichment in the deeper parts. Based on age and extension constrains for the geothermal system, the average rates of mineralization were estimated as follows, total sulphur: 1653 tonne/yr, sulphide: 700 tonne/yr, sulphate: 315 tonne/yr and carbon: 1054 tonne/yr over the life time of the system taken to be 20000 years.

References

Arnórsson, S. and Stefánsson, A., 1999. Assessment of feldspar solubility constants in water in the range 0 to 350 °C at vapor saturation pressures. Amer. J. Sci. 299, 173-209.

Arnórsson, S., 1978. Major element chemistry of geothermal sea-water at Reykjanes and Svartsengi, Iceland. Min. Mag., 42, 209-220.

Arnórsson, S., 1983. Chemical equilibria in Icelandic geothermal systems - implications for chemical geothermometry investigations. Geothermics 12, 119-128.

Arnórsson, S., 1995. Geothermal systems in Iceland: Structure and conceptual models. 1. High-temperature areas. Geothermics 24, 561-602.

Arnórsson, S., 1997. Interpretation of chemical and isotopic data on fluids discharged from wells in the Momotombo geothermal field, Nicaragua. International Atomic Energy Agency, Report NIC/8/008-04.

Arnórsson, S., Gunnlaugsson, E. and Svavarsson, H., 1983. The chemistry of geothermal waters in Iceland. 2. Mineral equilibria and independent variables controlling water compositions. Geochim. Cosmochim. Acta 47, 547-566.

Arnórsson, S., Stefánsson, A. and Bjarnason, J.Ö., 2007. Fluid-fluid interactions in geothermal systems. , Rev. Min. Geochem. 65, 259-312.

Barnes, H.L., 1979. Solubilities of ore minerals. In: Geochemistry of hydrothermal ore deposits, Barnes, H.L. (Ed.). New York, John Wiley&Sons, 404-460.

Bjarnason, J.Ö., 1994. The speciation program WATCH version 2.1. Icelandic National Authority Report.

Björnsson, S., Arnórsson, S. and Tómasson, J., 1970. Exploration of the Reykjanes thermal brine area. Geothermics 56, 2380-2391.

Björnsson, S., Arnórsson, S. and Tómasson, J., 1972. Economic evaluation of the Reykjanes thermal brine area, Iceland. Bull. Am. Assoc. Petrol. Geol. 56, 2380-2391.

Bödvarsson, G., 1961. Physical characteristics of natural heat resources in Iceland. Jökull 11, 29-38.

Browne, P.R.L., 1978. Hydrothermal alteration in active geothermal fields. Ann. Rev. Earth Planet. Sci. 6, 229-250.

Bruland, K.W., 1983. Trace elements in seawater. In: Chemical oceanography. Riley, J.P. and Chester, R. (Eds), Academic Press London, London. 8, 157-220.

Chelnokov, G., 2004. Interpretation of geothermal fluid compositions from Mendelev volcano, Kunashir, Russia. The United Nations University Geothermal Training Programme, Report 2004, 57-82.

D'Amore, F., Giusti, D. and Abdallah, A., 1998. Geochemistry of the high-salinity geothermal field of Asal, Republic of Djibouti, Africa. Geothermics 27, 197-210.

Ellis, A. and Mahon, W., 1977. Chemistry and geothermal systems. Academic Press, New York.

Ellis, A., 1970. Quantitative interpretation of chemical characteristics of hydrothermal systems. Geothermics 2, 516-528.

Ellis, A.J. and Mahon, W.A.J., 1964. Natural hydrothermal systems and experimental hot water/rock interactions, Part I. Geochim. Cosmochim. Acta 28, 1323-1357.

Ellis, A.J. and Mahon, W.A.J., 1967. Natural hydrothermal systems and experimental hot water/rock interactions, Part II. Acta 31. Geochim. Cosmochim. Acta 31, 519-538.

Flower, M.F.J., Pritchard, R.G., Brem, G., Cann, J.R., Delaney, J., Emmerman, R., Gibson, I.L., Oakley, P.J., Robinson, P.T., and Schmincke, H.U., 1982. Chemical stratiography, Iceland Research drilling project Reydarfjordur, Eastern Iceland. J. Geophys. Res 87, 6489-6510.

Fournier, R.O., 1985. Carbonate transport and deposition in the epithermal environment. Reviews in Econ. Geol. 2, 63-71.

Franzson, H., Thordason, S., Bjornsson, G., Gudlaugsson, S.T., Richter, B., Fridleifsson, G.O. and Thorhallsson, S., 2002. Reykjanes high-temperature field, SW-Iceland. Geology and hydrothermal alteration of well RN-10. Proceedings, 27th Workshop on GeothermalReservoir Engineering. Stanford University. 233–240.

Freedman, A.J.E., Bird, D.K., Arnórsson, S., Fridriksson, T., Elders, W.A. and Fridleifsson, G.O., 2009. Hydrothermal minerals record CO_2 partial pressures in the Reykjanes geothermal system, Iceland. Amer. J. Sci. 309, 788-833.

Fridleifsson, G.O. and Elders, W.A., 2005. The Iceland deep drilling project: a search for deep unconventional geothermal resources. Geothermics 34, 269-285.

Fridleifsson, G.Ó., 1991. Geothermal systems and associated alteration in Iceland. Geol. Surv. Jap. Report 277, 83-90.

Fridriksson, T., Kristjánsson, B.R., Ármannsson, H., Margrétardóttir, E., Olafsdóttir, S. and Chiodini, G., 2006. CO_2 emissions and heat flow through soil, fumaroles, and steam heated mud pools at the Reykjanes geothermal area, SW Iceland. Appl. Geochem. 21, 1551-1569.

Giggenbach, W.F., 1980. Geothermal gas equilibria. Geochim. Cosmochim. Acta 44, 2021-2032.

Giggenbach, W.F., 1981. Geothermal mineral equilibria. Geochim. Cosmochim. Acta 45, 393-410.

Giggenbach, W.F., 1992. Isotopic shifts in waters from geothermal and volcanic systems along convergent plate boundaries and their origin. Earth Plan. Sci. Lett. 113, 495-510.

Giroud, N., 2008. A chemical study of arsenic, boron and gases in high-temperature geothermal fluids in Iceland. Ph.D. thesis, Univ. Iceland, 110 pp.

Goff, F. and Janik, C., 2000. Geothermal systems. In: Encyclopedia of volcanoes, Sigurdsson H. (Ed.) Pergamon Press: 817-834.

Gudmundsson, B.Th. and Arnórsson, S., 2002. Geochemical monitoring of the Krafla and Námafjall geothermal areas, N-Iceland. Geothermics 31, 195-243.

Gudmundsson, J.S. and Thórhallsson, S., 1986. The Svartsengi reservoir in Iceland. Geothermics 15, 3-15.

Gunnarsson, I. and Arnórsson, S., 2000. Amorphous silica solubility and the thermodynamic properties of H_4SiO_4 degrees in the range of 0 to 350°C at Psat. Geochim. Cosmochim. Acta 64, 2295-2307.

Gunnlaugsson, E., 1977. The origin and distribution of sulphur in fresh and geothermally altered rocks in Iceland. Ph.D. thesis, Univ. Leeds, U.K., 192 pp.

Hardardóttir, V., Brown, K.L., Fridriksson, T., Hedenquist, J.W., Hannington, M.D. and Thorhallsson, S., 2009. Metals in deep liquid of the Reykjanes geothermal system, southwest Iceland: Implications for the composition of seafloor black smoker fluids. Geology 37, 1103-1106.

Hardardóttir, V., Hannington, M., Hedenquist, J., Kjarsgaard, I. and Hoal, K., 2010. Cu-Rich scales in the Reykjanes geothermal system, Iceland. Econ. Geol. 105, 1143-1155.

Hardardóttir, V., Kristmannsdóttir, H. and Ármannsson, H., 2001. Scale formation in wells RN-9 and RN-8 in the Reykjanes geothermal field, Iceland. In Water-Rock Interaction 10, Cidu, R. (Ed.). Balkema, 851–854.

Hedenquist, J.W. and Lowenstern, J.B., 1994. The role of magmas in the formation of hydrothermal ore-deposits. Nature 370, 519-527.

Helgeson, H.C., 1970. A chemical and thermodynamic model of ore deposition in hydrothermal systems. Min. Soc. Amer. Spec. Pap. 3, 155-186.

Holland, H.D. and Malinin, S.D., 1979. The solubility and occurrence of non-ore minerals. In: Geochemistry of hydrothermal ore deposits, Barnes, H.L. (Ed.), New York, John Wiley&Sons, 461-508.

Jakobsson, S., Jónsson, J. and Shido, F., 1978. Petrology of the western Reykjanes peninsula, Iceland. J. Petrol. 19, 669-705.

Johnson, J.W., Oelkers, E.H., Helgeson, H.C., 1992. SUPCRT92. A software package for calculating the standard molal thermodynamic properties of minerals, gases, aqueous species, and reactions from 1 to 5000 bar and 0 to 1000°C. Computer Geoscience 18, 899-947.

Kristmannsdóttir, H., 1975. Hydrothermal alteration of basaltic rocks in Icelandic geothermal areas. In 2nd U.N. Symp. Develop. Use of Geothermal Resources, Vol. 1, pp. 441-445. San Fancisco, CA.

Kristmannsdóttir, H., 1976. Types of clay minerals in hydrothermally altered basaltic rocks, Reykjanes, Iceland, National Energy Authority, Reykjavík.

Kristmannsdóttir, H., 1979. Alteration of basaltic rocks by geothermal activity at 100-300°C. In: Mortland, M., Farmer, V., (Eds.), Developments in Sedimentology. Elsevier, Amsterdam, 359-367.

Li, Y.H., 1982. A brief discussion on the mean oceanic residence time of elements. Geochim. Cosmochim. Acta 46, 2671-2675.

Lonker, S.W., Franzson, H. and Kristmannsdóttir, H., 1993. Mineral-fluid interactions in the Reykjanes and Svartsengi geothermal systems, Iceland. Amer. J. Sci. 293, 605-670.

Marini, L., 2006. Geological sequestration of carbon dioxide - thermodynamics, kinetics, and reaction path modeling. Volume 11, 1-453.

Marks, N., Schiffman, P., Zierenberg, R.A., Frannon, H. and Fridleifsson, G.O., 2010. Hydrothermal alteration in the Reykjanes geothermal system: Insights from Iceland deep drilling program well RN-17. J. Vol. Geotherm. Res. 189, 172-190.

Mountain, B.W. and Seward, T.M., 2003. Hydrosulfide/sulfide complexes of copper(I): Experimental confirmation of the stoichiometry and stability of $Cu(HS)_2^-$ to elevated temperatures. Geochim. Cosmochim. Acta 67, 3005-3014.

Nicholson, K., 1993. Geothermal fluids chemistry and exploration techniques. Springer-Verlag, Berlin.

Oelkers, E.H. and Gíslason, S.R., 2001. The mechanism, rates and consequences of basaltic glass dissolution: I. An experimental study of the dissolution rates of basaltic glass as a function of aqueous Al, Si and oxalic acid concentration at 25 °C and pH = 3 and 11. Geochim. Cosmochim. Acta 65, 3671-3681.

Pálmason, G., Johnsen, G.V., Torfason, H., Saemundsson, K., Ragnars, K., Haraldsson, G.I. and Halldórsson, G.K., 1985. Assessment of geothermal energy in Iceland. Orkustofnun Report, OS-85076/JHD-10.

Parkhurst, D.L. and Appelo, C.A.J., 1999. User´s guide to PHREEQC (Version 2) - A computer program for speciation, batch reaction, one-dimensional transport and inverse geochemical calculations. U.S. Geological Survey Water-Resources Investigations Report 99-4259, 310 pp.

Peate, D.W., Baker, J.A., Jakobsson, S.P., Waight, T.E., Kent, A.J.R., Grassineau, N.V. and Skovgaard, A.C., 2009. Historic magmatism on the Reykjanes Peninsula, Iceland: a snap-shot of melt generation at a ridge segment. Cont. Min. Petrol.157, 359-382.

Pokrovski, G.S. and Dubrovinsky, L.S., 2011. The S3- ion is stable in geological fluids at elevated temperatures and pressures. Science 331, 1052-1054.

Pope, E.C., Bird, D.K., Arnórsson, S., Fridriksson, T., Elders, W.A. and Fridleifsson, G.O., 2009. Isotopic constraints on ice age fluids in active geothermal systems: Reykjanes, Iceland. Geochim. Cosmochim. Acta 73, 4468-4488.

Ragnarsdóttir, K.V., Walther, J.V. and Arnórsson, S., 1984. Description and interpretation of the composition of fluid and alteration mineralogy in the geothermal system, at Svartsengi, Iceland. Geochim. Cosmochim. Acta 48, 1535-1553.

Renderos, R.E., 2009. Carbon dioxide fixation by calcite and diffusive degassing in the southern region of the Berlín geothermal system, El Salvador. M.Sc. Thesis, Faculty of Earth Sciences, University of Iceland, 54pp.

Saunier, S., 2011. Etude expérimentale du fractionnement isotopique du fer aux conditions hydrothermales. PhD thesis. Université Toulouse III - Paul Sabatier.

Schiffman, P., Fridleifsson, G.Ó., 1991. The smectite-chlorite transition in drillhole NH-15 Nesjavellir geothermal field, Iceland: XRD, BSE and electron microscope investigations. J. Metamorph. Geol. 9, 679-696.

Sigvaldason, G.E. and Elísson, G., 1968. Collection and analysis of volcanic gases at Surtsey. Iceland. Geochim. Cosmochim. Acta 32, 797-80.

Simmons, S.F. and Christenson, B.W., 1994. Origins of calcite in a boiling geothermal system. Amer. J. Sci. 294, 361-400.

Stefánsson, A. and Arnórsson, S., 2000. Feldspar saturation state in natural waters. Geochim. Cosmochim. Acta 64, 2567-2584.

Stefánsson, A. and Arnórsson, S., 2002. Gas pressures and redox reactions in geothermal fluids in Iceland. Chem. Geol. 190, 251-271.

Stefánsson, A. and Seward, T.M., 2003a. Experimental determination of the stability and stoichiometry of sulphide complexes of silver(I) in hydrothermal solutions to 400 °C. Geochim. Cosmochim. Acta 67, 1395-1413.

Stefánsson, A. and Seward, T.M., 2003b. The hydrolysis of gold(I) in aqueous solutions to 600 °C and 1500 bar. Geochim. Cosmochim. Acta 67, 1677-1688.

Stefánsson, A. and Seward, T.M., 2003c. Stability of chloridogold(I) complexes in aqueous solutions from 300 to 600 °C and from 500 to 1800 bar. Geochim. Cosmochim. Acta 67, 4559-4576.

Stefánsson, A. and Seward, T.M., 2004. Gold(I) complexing in aqueous sulphide solutions to 500 °C at 500 bar. Geochim. Cosmochim. Acta 68, 4121-4143.

Stefánsson, A., Arnórsson, S., Gunnarsson, I. and Kaasalainen, H., 2009. Sequestration of H_2S from the Hellisheidi power plant - a geochemical study. Sci. Inst. Report RH-14-2009. 84 pp.

Stefánsson, A., Arnórsson, S., Gunnarsson, I., Kaasalainen, H. and Gunnlaugsson, E., 2011. The geochemistry and sequestration of H_2S into the geothermal system at Hellisheidi, Iceland. J. Volc. Geotherm. Res. 202, 179-188.

Sveinbjörnsdóttir, A.E., Coleman, M.L. and Yardley, B.W.D., 1986. Origin and history of hydrothermal fluids of the Reykjanes and Krafla geothermal fields, Iceland - a stable isotope study. Cont. Min. Petrol. 94, 99-109.

Tagirov, B.R. and Seward, T.M., 2010. Hydrosulfide/sulfide complexes of zinc to 250 °C and the thermodynamic properties of sphalerite. Chem. Geol. 269, 301-311.

Tómasson, J. and Kristmannsdóttir, H., 1972. High-temperature alteration minerals and thermal brines, Reykjanes, Iceland. Cont. Min. Petrol. 36, 123-134.

Wiese, F., Fridriksson, T. and Ármannsson, H., 2008. CO_2 fixation by calcite in high-temperature geothermal systems in Iceland. Report prepared for Rannís, Hitaveita Sudurnesja hf., Orkuveita Reykjavíkur, Landsvirkjun and Orkustofnun, 35 pp.

Weissberg, B.G., Browne, P.R.L. and Seward, T.M., 1979. Ore metals in active geothermal systems. In: Geochemistry of hydrothermal ore deposits, Barnes, H.L. (Ed.), New York, John Wiley&Son, 738-780.

White, D.E., Muffler, L.J.P. and Truesdel, A., 1971. Vapor-dominated hydrothermal systems compared with hot-water systems. Eco. Geol. 66, 75-97.

Appendix A

Aqueous speciation using the llnl.dat database (log activity).

t/°C	pH	Na^+	H_4SiO_4	$Al(OH)_4^-$	K^+	Ca^{2+}	SO_4^{2-}	H^+	HCO_3^-	CO_2(aq)	H_2(aq)	H_2S(aq)	Mg^{2+}	Fe^{2+}	$Fe(OH)_4^-$	CH_4(aq)
310	4.74	-0.93	-1.96	-6.89	-1.94	-3.23	-6.29	-4.74	-4.98	-1.20	-4.15	-2.61	-6.42	-6.78	-23.24	-4.70
310	4.71	-0.94	-1.92	-7.06	-1.97	-3.23	-6.23	-4.71	-5.08	-1.27	-4.33	-2.58	-6.46	-6.94	-23.45	-5.16
310	4.88	-0.94	-1.91	-7.01	-1.95	-3.23	-6.26	-4.88	-4.95	-1.31	-4.10	-2.67	-6.42	-7.02	-23.05	-4.86
310	4.81	-0.94	-1.88	-7.37	-1.97	-3.21	-6.21	-4.81	-4.97	-1.26	-4.03	-2.59	-6.45	-7.27	-23.49	-4.77
295	4.86	-0.92	-1.95	-6.73	-1.95	-3.14	-6.16	-4.86	-4.90	-1.32	-4.45	-2.81	-6.48	-7.24	-23.32	-4.88
295	4.91	-0.92	-1.93	-7.17	-1.95	-3.13	-6.07	-4.91	-4.88	-1.34	-4.30	-2.88	-6.56	-7.66	-23.58	-5.12
295	4.92	-0.94	-1.98	-7.22	-1.97	-3.13	-6.01	-4.92	-4.91	-1.38	-4.53	-2.92	-6.62	-7.58	-23.46	-5.30
295	4.95	-0.93	-1.96	-6.92	-1.96	-3.12	-6.01	-4.95	-4.90	-1.41	-4.62	-2.95	-6.56	-7.53	-23.32	-5.36
295	4.96	-0.93	-1.96	-6.50	-1.96	-3.14	-5.98	-4.96	-4.88	-1.39	-4.62	-2.91	-6.43	-7.99	-23.75	-5.36
295	4.98	-0.93	-1.95	-6.64	-1.96	-3.15	-6.01	-4.98	-4.90	-1.43	-4.68	-3.14	-6.46	-7.44	-23.11	-5.16
285	4.92	-0.87	-2.00	-6.65	-1.92	-3.02	-5.91	-4.92	-4.85	-1.47	-4.06	-3.00	-6.58	-7.79	-23.64	-5.43
285	4.97	-0.88	-1.98	-6.68	-1.93	-3.02	-5.88	-4.97	-4.95	-1.61	-4.62	-3.05	-6.63	-7.50	-23.21	-5.72
275	4.95	-0.84	-1.99	-6.81	-1.90	-2.94	-5.73	-4.95	-4.75	-1.54	-4.11	-3.04	-6.44	-7.94	-23.69	-5.43
275	4.97	-0.85	-2.01	-6.62	-1.90	-2.91	-5.66	-4.97	-4.81	-1.62	-4.48	-3.09	-6.38	-7.30	-22.98	-5.92
285	4.96	-0.88	-2.00	-6.90	-1.94	-3.05	-5.84	-4.96	-4.79	-1.45	-4.02	-2.95	-6.56	-8.06	-23.81	-5.36
284	4.86	-0.87	-1.99	-6.50	-1.91	-3.01	-5.94	-4.86	-4.99	-1.56	-4.15	-2.99	-6.44	-7.44	-23.48	-5.51
305	4.96	-0.92	-1.93	-6.49	-1.94	-3.20	-6.14	-4.96	-5.01	-1.45	-3.78	-2.72	-6.36	-7.02	-22.82	-5.09
305	4.93	-0.95	-1.93	-7.13	-1.98	-3.24	-5.80	-4.93	-4.98	-1.39	-4.36	-2.74	-6.61	-7.37	-23.21	-5.51
285	4.60	-0.90	-1.99	-7.15	-1.95	-3.01	-6.04	-4.60	-4.99	-1.29	-4.33	-2.78	-6.43	-7.36	-24.14	-5.25
276	4.48	-0.89	-2.01	-6.91	-1.95	-2.93	-5.80	-4.48	-4.90	-1.20	-4.15	-2.83	-6.21	-7.37	-24.44	-5.03

Aqueous speciation using the wateqf.dat database (log activity).

t/°C	pH	Na^+	H_4SiO_4	$Al(OH)_4^-$	K^+	Ca^{2+}	SO_4^{2-}	H^+	HCO_3^-	CO_2(aq)	H_2(aq)	H_2S(aq)	Mg^{2+}	Fe^{2+}	$Fe(OH)_4^-$	CH_4(aq)
310	4.74	-0.78	-1.90	-6.13	-1.89	-2.89	-5.77	-4.74	-4.91	-1.21	-4.17	-2.55	-5.66	-5.61	-10.81	-4.64
310	4.71	-0.79	-1.86	-6.30	-1.92	-2.89	-5.71	-4.71	-5.01	-1.29	-4.35	-2.52	-5.70	-5.81	-11.08	-5.11
310	4.88	-0.78	-1.85	-6.30	-1.90	-2.88	-5.74	-4.88	-4.87	-1.33	-4.12	-2.61	-5.66	-5.86	-10.65	-4.81
310	4.81	-0.79	-1.82	-6.64	-1.92	-2.88	-5.68	-4.81	-4.89	-1.28	-4.04	-2.54	-5.70	-6.19	-11.16	-4.72
295	4.86	-0.76	-1.89	-6.02	-1.89	-2.82	-5.64	-4.86	-4.84	-1.34	-4.46	-2.75	-5.75	-6.10	-11.04	-4.82
295	4.91	-0.77	-1.87	-6.48	-1.90	-2.81	-5.55	-4.91	-4.81	-1.36	-4.32	-2.82	-5.82	-6.54	-11.31	-5.07
295	4.92	-0.79	-1.93	-6.55	-1.92	-2.83	-5.48	-4.92	-4.84	-1.40	-4.55	-2.87	-5.90	-6.59	-11.32	-5.25
295	4.95	-0.78	-1.91	-6.25	-1.90	-2.81	-5.48	-4.95	-4.83	-1.42	-4.64	-2.89	-5.83	-6.48	-11.12	-5.30
295	4.96	-0.78	-1.90	-5.83	-1.90	-2.82	-5.46	-4.96	-4.81	-1.41	-4.64	-2.85	-5.68	-6.89	-11.51	-5.30
295	4.98	-0.77	-1.89	-5.98	-1.90	-2.82	-5.49	-4.98	-4.83	-1.45	-4.70	-3.09	-5.71	-6.30	-10.83	-5.10
285	4.92	-0.72	-1.94	-6.00	-1.86	-2.73	-5.41	-4.92	-4.80	-1.49	-4.08	-2.94	-5.88	-6.70	-11.64	-5.37
285	4.97	-0.73	-1.92	-6.05	-1.87	-2.74	-5.38	-4.97	-4.89	-1.63	-4.64	-2.98	-5.93	-6.44	-11.25	-5.66
275	4.95	-0.70	-1.93	-6.21	-1.85	-2.70	-5.27	-4.95	-4.71	-1.56	-4.13	-2.98	-5.81	-7.01	-12.09	-5.37
275	4.97	-0.71	-1.95	-6.03	-1.85	-2.67	-5.19	-4.97	-4.77	-1.64	-4.50	-3.03	-5.73	-6.32	-11.33	-5.86
285	4.96	-0.74	-1.95	-6.27	-1.88	-2.78	-5.34	-4.96	-4.74	-1.46	-4.04	-2.89	-5.87	-7.09	-11.93	-5.30
284	4.86	-0.72	-1.92	-5.84	-1.85	-2.72	-5.44	-4.86	-4.93	-1.57	-4.16	-2.93	-5.74	-6.36	-11.51	-5.45
305	4.96	-0.76	-1.87	-5.78	-1.88	-2.85	-5.61	-4.96	-4.93	-1.47	-3.80	-2.66	-5.60	-5.82	-10.36	-5.03
305	4.93	-0.79	-1.88	-6.43	-1.92	-2.89	-5.29	-4.93	-4.90	-1.40	-4.38	-2.69	-5.82	-6.23	-10.82	-5.45
285	4.60	-0.76	-1.93	-6.41	-1.90	-2.75	-5.53	-4.60	-4.94	-1.31	-4.35	-2.73	-5.76	-6.43	-12.29	-5.20
276	4.48	-0.76	-1.96	-6.15	-1.89	-2.71	-5.32	-4.48	-4.85	-1.22	-4.17	-2.78	-5.59	-6.56	-12.94	-4.98

Appendix B

The reaction quotients for selected minerals using the llnl.dat database.

t/°C	pH	l-alb	mic	qtz	anh	cc	chl	czo	epi	wol	pre	py	wai	mt	gro	pyrr
310	4.74	-13.69	-14.70	-1.96	-9.53	-3.48	-13.88	-28.28	-44.62	4.28	-16.65	1.63	-24.84	-53.25	-10.42	0.08
310	4.71	-13.75	-14.77	-1.92	-9.46	-3.60	-14.48	-28.68	-45.08	4.27	-16.91	1.66	-25.01	-53.84	-10.72	-0.10
310	4.88	-13.66	-14.68	-1.91	-9.49	-3.30	-12.78	-28.31	-44.36	4.63	-16.42	1.50	-24.86	-53.12	-9.89	0.08
310	4.81	-13.94	-14.97	-1.88	-9.42	-3.36	-14.10	-29.35	-45.47	4.54	-17.17	1.20	-25.46	-54.25	-10.75	-0.23
295	4.86	-13.48	-14.52	-1.95	-9.30	-3.19	-12.84	-27.45	-44.04	4.63	-15.86	1.30	-24.39	-53.87	-9.29	-0.34
295	4.91	-13.88	-14.91	-1.93	-9.20	-3.10	-13.67	-28.65	-45.06	4.75	-16.57	0.70	-25.19	-54.82	-9.89	-0.72
295	4.92	-14.10	-15.13	-1.98	-9.14	-3.12	-14.15	-28.95	-45.19	4.72	-16.81	0.93	-25.49	-54.50	-10.11	-0.67
295	4.95	-13.73	-14.76	-1.96	-9.14	-3.07	-12.92	-27.93	-44.33	4.82	-16.06	1.09	-24.80	-54.17	-9.28	-0.58
295	4.96	-13.30	-14.33	-1.96	-9.13	-3.06	-11.31	-26.69	-43.94	4.82	-15.23	0.73	-23.97	-55.48	-8.45	-0.98
295	4.98	-13.42	-14.45	-1.95	-9.16	-3.06	-11.59	-27.09	-43.56	4.87	-15.46	0.92	-24.23	-53.67	-8.65	-0.62
285	4.92	-13.52	-14.56	-2.00	-8.93	-2.95	-12.80	-27.06	-44.05	4.83	-15.49	0.12	-24.31	-55.07	-8.66	-0.95
285	4.97	-13.51	-14.56	-1.98	-8.90	-3.00	-12.73	-27.07	-43.60	4.93	-15.42	0.97	-24.31	-53.92	-8.51	-0.61
275	4.95	-13.61	-14.67	-1.99	-8.67	-2.74	-12.22	-27.31	-44.19	4.97	-15.56	0.00	-24.50	-55.32	-8.60	-1.08
275	4.97	-13.50	-14.55	-2.01	-8.57	-2.75	-11.42	-26.74	-43.10	5.02	-15.15	0.94	-24.19	-53.26	-8.12	-0.45
285	4.96	-13.78	-14.84	-2.00	-8.89	-2.89	-12.93	-27.85	-44.76	4.86	-15.99	-0.03	-24.85	-55.69	-9.13	-1.10
284	4.86	-13.33	-14.37	-1.99	-8.95	-3.14	-12.29	-26.62	-43.60	4.72	-15.26	0.43	-23.95	-54.40	-8.55	-0.72
305	4.96	-13.20	-14.22	-1.93	-9.34	-3.24	-10.86	-26.68	-43.02	4.80	-15.23	1.24	-23.90	-52.66	-8.50	0.18
305	4.93	-13.88	-14.90	-1.93	-9.04	-3.28	-13.67	-28.72	-44.80	4.69	-16.67	1.37	-25.22	-53.78	-10.04	-0.25
285	4.60	-14.01	-15.07	-1.99	-9.05	-3.40	-15.59	-28.83	-45.82	4.20	-17.08	0.60	-25.26	-55.64	-10.89	-0.94
276	4.48	-13.84	-14.89	-2.01	-8.73	-3.35	-15.08	-28.14	-45.68	4.01	-16.75	0.08	-24.80	-56.26	-10.73	-1.25

The reaction quotients for selected minerals using the wateq4f.dat database

t/°C	pH	l-alb	mic	qtz	anh	cc	chl	czo	epi	wol	pre	py	wai	mt	gro	pyrr
310	4.74	-12.60	-13.71	-1.90	-8.66	-3.06	-8.40	-25.13	-29.81	4.68	-14.26	2.94	-22.74	-27.23	-7.68	1.32
310	4.71	-12.66	-13.79	-1.86	-8.61	-3.19	-9.01	-25.55	-30.32	4.67	-14.54	2.91	-22.93	-27.96	-8.01	1.09
310	4.88	-12.62	-13.74	-1.85	-8.62	-2.88	-7.40	-25.31	-29.67	5.03	-14.14	2.79	-22.86	-27.17	-7.25	1.29
310	4.81	-12.89	-14.02	-1.82	-8.57	-2.96	-8.75	-26.34	-30.86	4.92	-14.88	2.41	-23.45	-28.51	-8.14	0.91
295	4.86	-12.45	-13.58	-1.89	-8.46	-2.79	-7.57	-24.51	-29.53	5.01	-13.63	2.58	-22.42	-28.18	-6.73	0.86
295	4.91	-12.86	-14.00	-1.87	-8.36	-2.71	-8.42	-25.77	-30.60	5.14	-14.38	1.96	-23.26	-29.16	-7.37	0.46
295	4.92	-13.12	-14.25	-1.93	-8.31	-2.75	-9.02	-26.18	-30.95	5.08	-14.71	2.06	-23.64	-29.23	-7.70	0.38
295	4.95	-12.74	-13.87	-1.91	-8.29	-2.69	-7.75	-25.13	-30.00	5.19	-13.93	2.28	-22.93	-28.73	-6.84	0.53
295	4.96	-12.31	-13.43	-1.90	-8.28	-2.66	-6.08	-23.88	-29.55	5.21	-13.08	1.97	-22.08	-29.90	-5.97	0.18
295	4.98	-12.42	-13.55	-1.89	-8.31	-2.66	-6.33	-24.26	-29.11	5.26	-13.30	2.19	-22.34	-27.96	-6.15	0.58
285	4.92	-12.54	-13.67	-1.94	-8.14	-2.60	-7.82	-24.35	-29.99	5.18	-13.43	1.35	-22.48	-29.98	-6.31	0.21
285	4.97	-12.55	-13.69	-1.92	-8.11	-2.66	-7.80	-24.43	-29.62	5.27	-13.41	2.16	-22.53	-28.94	-6.22	0.51
275	4.95	-12.70	-13.85	-1.93	-7.97	-2.46	-7.66	-24.88	-30.76	5.26	-13.72	1.06	-22.84	-31.20	-6.53	-0.09
275	4.97	-12.59	-13.73	-1.95	-7.85	-2.46	-6.79	-24.31	-29.60	5.32	-13.31	2.06	-22.53	-28.98	-6.03	0.59
285	4.96	-12.84	-13.98	-1.95	-8.12	-2.56	-8.05	-25.24	-30.90	5.19	-14.02	1.09	-23.09	-30.94	-6.88	-0.06
284	4.86	-12.33	-13.46	-1.92	-8.17	-2.80	-7.32	-23.88	-29.55	5.06	-13.19	1.66	-22.10	-29.38	-6.20	0.43
305	4.96	-12.15	-13.27	-1.87	-8.46	-2.82	-5.44	-23.68	-28.26	5.21	-12.94	2.59	-21.89	-26.54	-5.86	1.45
305	4.93	-12.86	-13.99	-1.88	-8.18	-2.86	-8.14	-25.78	-30.17	5.10	-14.42	2.63	-23.27	-27.88	-7.44	0.94
285	4.60	-12.97	-14.11	-1.93	-8.29	-3.09	-10.61	-25.93	-31.81	4.51	-14.92	1.67	-23.31	-31.00	-8.47	0.05
276	4.48	-12.81	-13.94	-1.96	-8.03	-3.09	-10.32	-25.29	-32.08	4.28	-14.66	1.01	-22.87	-32.44	-8.42	-0.38

Appendix C

Sulphides, sulphates, total sulphur and total carbon content in drill cuttings from well RN-10. Concentrations are in wt% and depth in m.

Depth	Sulphides	Sulphates	Total S	Total C
100	0.020	1.760	1.780	0.041
150	0.919	0.230	1.149	0.541
202	0.646	0.047	0.693	0.773
252	0.559	0.032	0.592	0.040
300	0.806	0.104	0.909	0.978
350	0.000	0.714	0.713	0.428
400	0.042	0.593	0.635	0.759
452	0.093	0.160	0.254	2.138
500	0.091	0.204	0.295	1.086
550	0.279	0.343	0.622	1.448
600	0.000	0.186	0.181	0.583
652	0.006	0.055	0.061	0.148
701	0.088	0.062	0.150	0.068
750	0.000	0.073	0.077	0.217
800	0.008	0.029	0.036	0.036
850	0.000	0.061	0.060	0.084
900	0.062	0.112	0.174	0.036
950	0.099	0.049	0.149	0.012
1002	0.032	0.041	0.074	0.011
1050	0.050	0.205	0.255	0.017
1100	0.169	0.053	0.222	0.000
1150	0.083	0.071	0.154	0.006
1200	0.021	0.053	0.075	0.000
1250	0.256	0.203	0.459	0.000
1302	0.062	0.048	0.110	0.003
1352	0.372	0.110	0.482	0.000
1400	0.056	0.082	0.138	0.005
1452	0.042	0.067	0.109	0.018
1500	1.027	0.225	1.251	0.027
1550	0.055	0.107	0.162	0.036
1600	0.064	0.056	0.120	0.016
1650	0.124	0.073	0.197	0.018
1700	0.075	0.057	0.132	0.012
1750	0.313	0.100	0.413	0.011
1800	0.029	0.043	0.072	0.011
1850	0.030	0.045	0.075	0.024
1900	0.314	0.120	0.435	0.016
1952	0.298	0.183	0.481	0.021
2004	0.037	0.162	0.199	0.034
2051	0.037	0.103	0.140	0.034

Sulphides, sulphates, total sulphur and total carbon content in drill cuttings from well RN-17. Concentrations are in wt% and depth in m.

Depth	Sulphides	Sulphates	Total S	Total C
100	0.184	0.152	0.335	0.428
150	1.164	0.250	1.413	0.874
200	0.196	0.167	0.363	1.082
250	0.260	0.107	0.367	0.488
300	0.125	0.247	0.372	0.761
350	0.025	0.090	0.115	0.287
400	0.019	0.344	0.362	0.408
500	0.061	0.095	0.156	0.178
550	0.915	0.177	1.092	0.043
650	0.516	0.216	0.732	0.204
700	0.000	0.027	0.028	0.048
750	0.026	0.053	0.079	0.060
800	0.009	0.085	0.094	0.034
850	0.067	0.032	0.100	0.048
950	0.118	0.086	0.205	0.038
1000	0.027	0.048	0.075	0.094
1050	0.011	0.049	0.060	0.026
1100	0.053	0.093	0.147	0.010
1150	0.000	0.140	0.144	0.003
1200	0.123	0.089	0.212	0.005
1300	0.031	0.115	0.146	0.001
1350	0.773	0.076	0.849	0.011
1400	0.039	0.068	0.106	0.001
1450	0.028	0.138	0.166	0.018
1550	0.040	0.026	0.065	0.005
1600	0.030	0.022	0.052	0.011
1700	0.065	0.031	0.095	0. 016
1800	0.652	0.095	0.747	0.000
1900	0.413	0.146	0.559	0.007
2000	0.087	0.045	0.132	0.000
2100	0.041	0.041	0.083	0.000
2200	0.109	0.038	0.147	0.000
2300	0.043	0.065	0.108	0.000
2400	0.103	0.064	0.166	0.000
2550	0.286	0.101	0.387	0.000
2650	0.238	0.097	0.335	0.000
2800	0.049	0.035	0.084	0.000
2900	0.123	0.097	0.219	0.000
2950	0.087	0.047	0.135	0.000
3050	0.052	0.074	0.126	0.000